Hydrological Study on Subsurface Temperature in Nagaoka Plain

Makoto TANIGUCHI

Hydrological Study on Subsurface Temperature in Nagaoka Plain

by

Makoto TANIGUCHI

A DISSERTATION

submitted in partial fulfilment of

the requirements for the degree of

DOCTOR OF SCIENCE

Institute of Geoscience

University of Tsukuba, Ibaraki, Japan

1986

TABLE OF CONTENTS

ACKNOWLEDGEMENTS

The author wishes to express his gratitude to his academic adviser, Professor Dr. Isamu Kayane, Institute of Geoscience, the University of Tsukuba, for his continuing guidance and encouragements during the graduate work and research. Special thanks are extended to Professor Dr. Shigemi Takayama, Professor Dr. Sizuo Shindo and Associate Professor Dr. Kazuo Kotoda, Institute of Geoscience, the University of Tsukuba, for their suggestions and guidance.

The author is grateful to Dr. Tadashi Tanaka, Dr. Yuichi Suzuki and Dr. Norio Tase, Institute of Geoscience, the University of Tsukuba, Dr. Yasuo Sakura, Department of Earth Sciences, Chiba University, and Dr. Akihiko Kondoh, Environmental Research Center, for their useful discussions.

In addition, thanks are also extended to Shinano-gawa Construction Office for his assistance in on-the-spot surveys and permission to use data of the Nagaoka region. Finally, the author wishes to express his thanks to all those who helped him in the course of his work.

ABSTRACT

The subsurface temperature, one of the most easily measurable and universal elements in groundwater survey, is a conservative quantity in a groundwater flow system. In this study, seasonal and secular variations of subsurface temperature in an alluvial plain are obtained by measuring the water temperature in wells. The relationship between the regional difference of subsurface temperature and regional groundwater flow rate by which the temperature difference is caused, is clarified.

The study area is located in Nagaoka City, Japan. The main aquifer is composed of a gravel-rich alluvial formation. The mean annual temperature and precipitation are 12.5 ℃ and 2654 mm, respectively. About 40 to 50 % of the precipitation is concentrated from November to February, mostly as snowfall.

Soil temperature, thermal conductivity of soil and soil water content were measured in the unsaturated zone, and groundwater temperature and groundwater level were measured in 32 observation wells and 30 shallow wells in the saturated zone. Snow depth and density were also measured. The observation period was from August 1982 to August 1985.

In the unsaturated zone, soil temperature falls during the snowmelt season in the daytime and recovers after that. This is caused by the movement of mobile water under the temperature gradient that is steep and positive downward, and by the exchange between soil particles plus immobile water

and mobile water.

In the saturated zone, temperature-depth profiles are classified into four characteristic types which were named as recharge, discharge, advection and pumping types. The depths to the isothermal layer of the recharge and discharge types are deeper and shallower by 5 m than the value calculated by heat conduction theory, respectively. These phenomena can be explained by the downward groundwater flow and by the upward groundwater flow of the order of 0.01 m/day throughout the year, respectively.

Temperature-depth profiles of advection and pumping types can be explained by the horizontal movement of induced water and by the downward shift of the warmer shallow water, respectively. Then, it was clarified that the infiltration rate in the recharge area is about two times as large as that in the discharge area and that the infiltration ratio of the snowmelt water is about 1.5 times as large as the that of rainfall.

LIST OF TABLES

LIST OF FIGURES

LIST OF SYMBOLS

Symbol	Definition
A	Amplitude of soil temperature at the surface
A_0	Soil temperature at the infinite depth
a	Volume coefficient of thermal expansion of the fluid
ai	Interfacial area per unit volume
C	Constant, equal to 216 in cgs units
c	Specific heat of the aquifer
c_0	Specific heat of the fluid
cs	Specific heat of the immobile water and soil particles
cw	Specific heat of the mobile water
E	Annual potential evapotranspiration
f_1	Solid ratio in the soil
f_2	Immobile water content
Gc	Critical gradient of water temperature
g	Acceleration due to gravity
h	Heat transfer coefficient
I	Infiltration rate
Kx	Hydraulic conductivity of the aquifer in x direction
Kz	Hydraulic conductivity of the aquifer in z direction
ks	Thermal conductivity of immobile water and soil particles
kw	Thermal conductivity of mobile water

kx	Thermal conductivity of the aquifer in x direction
ky	Thermal conductivity of the aquifer in y direction
kz	Thermal conductivity of the aquifer in z direction
N	Ratio of the coefficient of viscosity
P	Annual precipitation
qx	Water flux in x direction
qy	Water flux in y direction
qz	Water flux in z direction
R	Annual recharge to the groundwater
Rs	Recharge to the groundwater from May to October
Rw	Recharge to the groundwater from November to April
R*	Sum of the deviation from annual mean of recharge to the groundwater
r	Radius of the well
S	Snowmelt rate
T	Temperature
Ta	Annual mean of air temperature
Tc	The lowest water temperature in the aquifer
Th	The highest water temperature in the aquifer
Ts	Temperature of immobile water and soil particles
Ts_0	Annual mean of ground surface temperature
Ts_3	Annual mean of soil temperature at the depth of 3 m
Tw	Temperature of mobile water

t	Time
Vz	Mobile water velocity in z direction
α	Thermal diffusivity of the fluid
αx	Thermal diffusivity of the aquifer in x direction
αy	Thermal diffusivity of the aquifer in y direction
αz	Thermal diffusivity of the aquifer in z direction
γc	Specific gravity of cold water
γh	Specific gravity of hot water
Θm	Mobile water content
μ	Coefficient of viscosity
ν	Kinematic viscosity of the fluid
ρ	Density of the aquifer
ρ_0	Density of the fluid
ρs	Density of the immobile water and soil particles
ρw	Density of the mobile water
ω	Period of surface temperature oscillation

I. INTRODUCTION

There are three methods to clarify the groundwater flow in a wide area which are the measuring of fluid potential, numerical simulation and the pursuing of tracer. It is difficult to observe continuously the fluid potential because of the deviation of depth and position of the wells and because of the expenses of many instrumentations. The methods of numerical simulation have many problems on establishing boundary conditions and determining the aquifer parameters. In contrast, the method using a tracer is effective because it is possible to estimate directly the groundwater flow from a tracer stored under water.

The tracers for a groundwater survey are classified based on detecting method into seven kinds, which are colorimetry, photometry, mass spectrograph, the methods for measuring electrical conductivity, chemical component, radioisotope (Todd, 1959) and temperature. Most of these tracers have many problems which are the adsorption of the soil particle and the necessity for a large amount of a tracer in a wide area. In the case of using the water quality of groundwater itself as a tracer, it is necessary to select a special one which is very different from surrounding water quality. Therefore, this method is lacking in universality. The method using tritium, the radioisotope of hydrogen, is applicable in a wide area as a tracer because the rainfall contained high density tritium caused by nuclear

tests. However, the quantitative analysis of tritium distribution has become difficult because the tritium concentration has been decreased due to radioactive decay. From the fact mentioned above, it can be seen that the groundwater temperature is one of the most useful tracers for the investigation of groundwater flow. This is because the method using water temperature has no problems on the adsorption and the amount of tracer, and because the physical treatment and measurement of water temperature are easy. In addition, the method using subsurface temperatures can be applied in the every region (Taniguchi et al., 1984). In this study, subsurface temperature is defined as the temperature which contains both soil temperature in the unsaturated zone and groundwater temperature in the saturated zone.

1-1 Previous studies

The heat conduction theory has been used to analyze the groundwater temperature in a wide area. When the heat is transported by heat conduction, the three-dimensional equation of heat conduction in the saturated zone is shown as follows:

$$\frac{\partial T}{\partial t} = \alpha x \frac{\partial^2 T}{\partial t^2} + \alpha y \frac{\partial^2 T}{\partial t^2} + \alpha z \frac{\partial^2 T}{\partial t^2} \qquad \text{.....(1)}$$

where T and t show the groundwater temperature and time, respectively. The αx, αy and αz show the thermal

diffusivities of the aquifer in the directions of x, y and z. If $T=A_0$ (°C) at $z=\infty$ when $t>0$ and the temperature at $z=0$ changes in the manner $T=A\sin\omega t$, the analytical solution of the one-dimensional heat conduction equation becomes as follows (Carslaw and Jaeger, 1959):

$$T(z,t) = A_0 + A\exp[-(\omega/2\alpha z)^{\frac{1}{2}}\cdot z]\cdot\sin[\omega t-(\omega/2\alpha z)^{\frac{1}{2}}\cdot z] \quad \cdots(2)$$

The study of groundwater temperatures considering both heat conduction and convection in the saturated zone, was started by Stallman (1963), who derived a theoretical equation of heat and fluid flow as follows:

$$c\rho\frac{\partial T}{\partial t} = kx\frac{\partial^2 T}{\partial t^2} + ky\frac{\partial^2 T}{\partial t^2} + kz\frac{\partial^2 T}{\partial t^2} - c_0\rho_0\left(qx\frac{\partial T}{\partial x} + qy\frac{\partial T}{\partial y} + qz\frac{\partial T}{\partial z}\right) \quad \cdots\cdots\cdots(3)$$

where $c\rho$ and $c_0\rho_0$ show the heat capacity of saturated soil and water, respectively. Furthermore, k and q indicate the thermal conductivity and water flux, and subscripts x, y and z denote the directions.

As for one-dimensional studies, Suzuki (1960) and Stallman (1965) derived an analytical solution of the partial differential equation. Bredehoeft and Papadopulos (1965) introduced a method to obtain the water flux in a steady state, by use of a type-curve. Cartwright (1970), Sorey (1971) and Sakura (1978) applied the method to the areas where the upward or downward flow dominates. Boyle and

Saleem (1979) and Cartwright (1979) showed the validity of the type-curve method by checking the water balance. As for two-dimensional studies, Parsons (1970) obtained a solution for the differential equations concerning heat and mass transfer in a steady state by a numerical analysis. Domenico and Palciauskas (1973) derived two-dimensional analytical solutions. In addition, the numerical analysis between the injection and withdrawal wells (Yokoyama et al., 1975), the horizontal flow model (Sakura, 1977), the model of soil temperature in a geothermal area (Yusa, 1981) and the mathematical model of the heat transport through the groundwater system in a thermal pollution area (Andrews and Anderson, 1979) have been proposed.

As for the subsurface temperature in Japan, Kiuchi (1950) obtained the temperature and depth to the isothermal layer. His conclusion is that the depth to the isothermal layer was from 12 m to 14 m with an exception of 10m in Hokkaido. After that, Yamaguchi (1966), Ohwada (1969) and Nishizawa and Hasegawa (1969) obtained the relationships between the mean annual air temperature and the temperature of the top of isothermal layer, or the mean annual soil temperature. Takahashi (1967) and Arai(1968) mentioned that the snow decreased the soil temperature on the side of the Sea of Japan, based on the distribution of subsurface temperature obtained from the studies mentioned above. Murashita (1968) inferred that the difference of subsurface temperature between the regions along the Sea of Japan and the Pacific Ocean was related to the rain-factor. However,

these studies do not deal with the process of heat transport by water movement.

Theoretical studies on heat and mass transport in the unsaturated zone have developed, for the most part from the work of Philip and De Vries (1957) and De Vries (1958). After that, Wilkinson and Klute (1962), Cary (1966), and Jury and Miller (1974) indicated the importance of the vapor transport. However, Kimball et al. (1976) and Higuchi (1978) showed that the vapor transport was negligible in wet soil. Recently, Sophocleous (1979) and Milly (1982) have rewritten the diffusion equations by using formulae based on the suction and temperature. On the other hand, there are some studies based on the fluid observations of soil temperature. Shul'gin (1957) studied the change in shallow soil temperature by snow cover. Sarson (1960) observed a soil temperature fall at the beginning of the snowmelt season. He observed temperature falls after the first of snowmelt season by 2 °C and 4.7 °C at the depths of 1.2m and 3m, respectively. Wierenga et al. (1970) clarified the soil temperature changes due to irrigation by warm or cold water. In Japan, Kobayashi (1979) indicated the soil temperature fall at the first of snowmelt season. Sakura (1984) observed the soil temperature change due to rainfall in an experimental plot. However, these observations are lacking in quantitative treatment of the subject.

Recently, it has become necessary to treat the mass transport problems by dividing the soil water into mobile and immobile waters (Van Genuchten and Wierenga, 1976;

Akratanakul et al., 1983; Trudgill et al., 1983; Smettem, 1984). However, this treatment has only been applied to the solute transport problem, not to the heat transport problem.

1-2 Objectives of this study

The subsurface temperature in a snowy area is lower than that in non-snowy areas even though the mean annual air temperature is the same. This suggests that heat conduction alone cannot explain the subsurface temperature and that heat convection by infiltrated meltwater may affect the subsurface temperature. Therefore, it is necessary to evaluate the effect of infiltration of snowmelt water on subsurface temperatures in a snowy area. In addition, it is necessary in the unsaturated zone to divide the soil water into mobile and immobile waters in heat transport problems as well as mass transport problems, considering the previous studies as mentioned in Section 1-1.

In the saturated zone, the groundwater temperature has been obtained from the water temperature measured at the bottom in the shallow wells as horizontal two-dimensional data. However, it is considered that the subsurface temperature is influenced by three-dimensional water flow. Therefore, it is necessary to clarify the three-dimensional distribution of groundwater temperature. In addition, it has been studied that subsurface temperature in Japan is affected by air temperature, snow cover and rain-factor and so on. However, their studies did not treat the problem

quantitatively and not pay attention to the typicality of subsurface temperatures in the groundwater flow system. That is to say, when the subsurface temperature corresponded to climatological conditions, the location of measuring the subsurface temperature is not considered, whether it was in the recharge area or discharge area, and so on. Therefore, it is necessary to clarify the regional difference of subsurface temperature in the basin, and to clarify the relationship between the temperature difference and the groundwater flow rate by which the difference is caused.

The objectives of this study are summarized as follows;

(1) to clarify the mechanism of heat transport in the soil during the infiltration of snowmelt water.

(2) to estimate the infiltration rate of snowmelt water, based on the changes in soil temperature.

(3) to indicate that the groundwater temperature field can be clarified by measuring water temperature in wells.

(4) to clarify the regional difference of subsurface temperature in the groundwater flow system.

(5) to clarify the relationship between regional difference of subsurface temperature and regional groundwater flow rate by which the difference is caused.

II. SUBSURFACE TEMPERATURE IN JAPAN

For the general perspective of regional distribution of subsurface temperature in Japan, preliminary analyses are made in this chapter by using the soil temperature measured at meteorological and agricultural stations (Ministry of Agriculture, Forestry and Fisheries and Meteorological Agency, 1982 and 1984).

2-1 Distribution of subsurface temperature

Routine measurements of soil temperatures in Japan were made from 1931 to 1970 at 104 points. Generally, the subsurface temperature at an arbitrary point changes with depth and time. For the representative values regarding subsurface temperature, the depth to the isothermal layer and the mean annual soil temperature at the depth of 3 m below the surface are selected in this chapter. This is because the profile of subsurface temperature in Japan is nearly vertical below the depth of 3 m.

Figure 1 shows the distribution of the mean annual soil temperature at the depth of 3m below the surface. It can be seen from this figure that the soil temperature decreases in proportion to the increasing latitude. The relationship between annual means of soil and air temperatures is shown by the equation as follows:

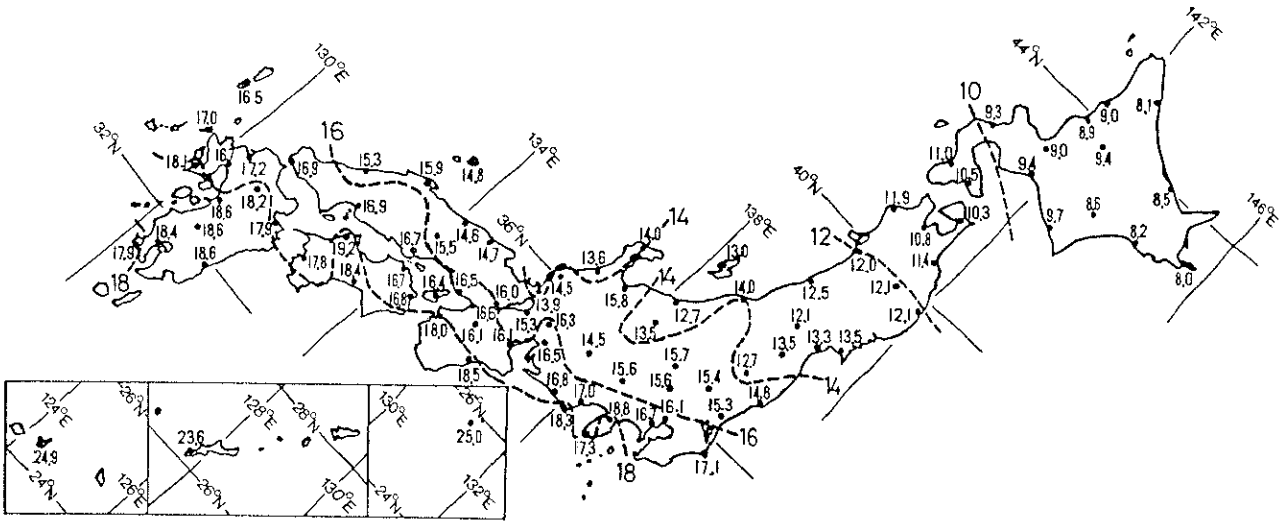

Figure 1 Distribution of T_{s3} (°C) in Japan.
T_{s3} : Mean annual soil temperature at the depth of 3 m.

$$Ts_3 = 0.956\ Ta + 2.156 \quad \text{.....(4)}$$

where Ts_3 and Ta show the soil temperature at the depth of 3m and air temperature, respectively. The isothermal lines of 14 °C and 16 °C overhang to the south in Hokuriku and San-in, respectively.

If it is assumed that the subsurface temperature is affected only by heat conduction, the difference between annual mean of subsurface temperature (Ts_3) and ground surface temperature (Ts_0) should be very small considering equation (2). In other words, the difference between Ts_3 and Ts_0 shows the effect of heat convection and so on. Figure 2 shows the distribution of $Ts_3 - Ts_0$ (Ts_0 shows the annual mean of ground surface temperature). The areas where $Ts_3 - Ts_0$ is negative are located in Tohoku, Hokuriku and San-in along the Sea of Japan. In contrast, the areas where $Ts_3 - Ts_0$ is large are located in Hokkaido, Izu Peninsula, Kii Peninsula, the south west of Shikoku and central Kyushu.

2-2 Depth to the isothermal layer

In this section, the estimation of the depth to the isothermal layer by exponential approximation is made using soil temperatures at the depths of 0.5, 1, 2, 3 and 5m below the surface. The depth at which the change in soil temperature decreases to 0.1 °C during a year is defined as the depth to the isothermal layer. Figure 3 shows the distribution of the depth to the isothermal layer in Japan

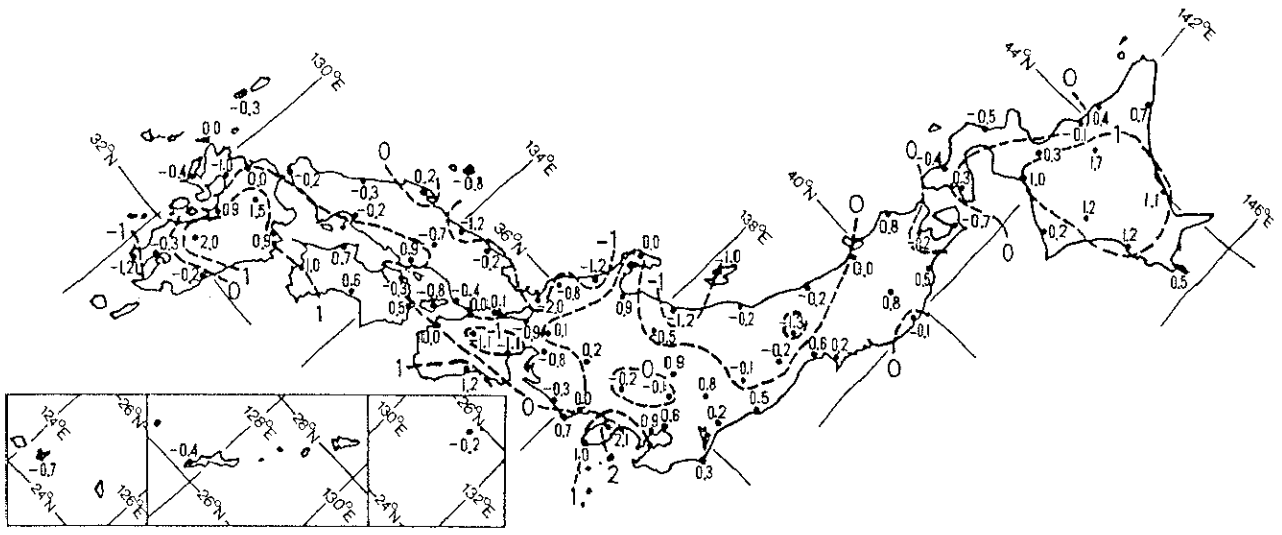

Figure 2 Distribution of $Ts_3 - Ts_0$ (°C) in Japan.
Ts_0 : Mean annual soil temperature at surface.

obtained by the method mentioned above. Though the distribution of the depth is complicated, the areas where the depth to the isothermal layer is deep are located along the Sea of Japan, in southern Kii Peninsula, western Shikoku and northern Kanto. In contrast, the areas where the depth is shallow, are located in eastern Hokkaido and northeastern Tohoku.

2-3 Distribution of recharge to the groundwater

If heat is transported only by heat conduction, the difference between Ts_3 and Ts_0 in Figure 2 should be very small. However, the distribution of $Ts_3 - Ts_0$ shows regional characteristics with positive and negative values. It suggests that heat convection contributes to the heat transport. Then, the monthly recharge to the groundwater which cause the heat convection is calculated. If the surface runoff can be negligible because the observation point is usually located in a flat field, the water balance at any point in the month, i, is shown as follows:

$$R_i = P_i - E_i \qquad \text{.....(5)}$$

where R is the recharge to the groundwater, and P and E show the precipitation and the actual evapotranspiration, respectively. As the estimation of the actual evapotranspiration from the climatological data is difficult, the potential evapotranspiration by the Thornthwaite method

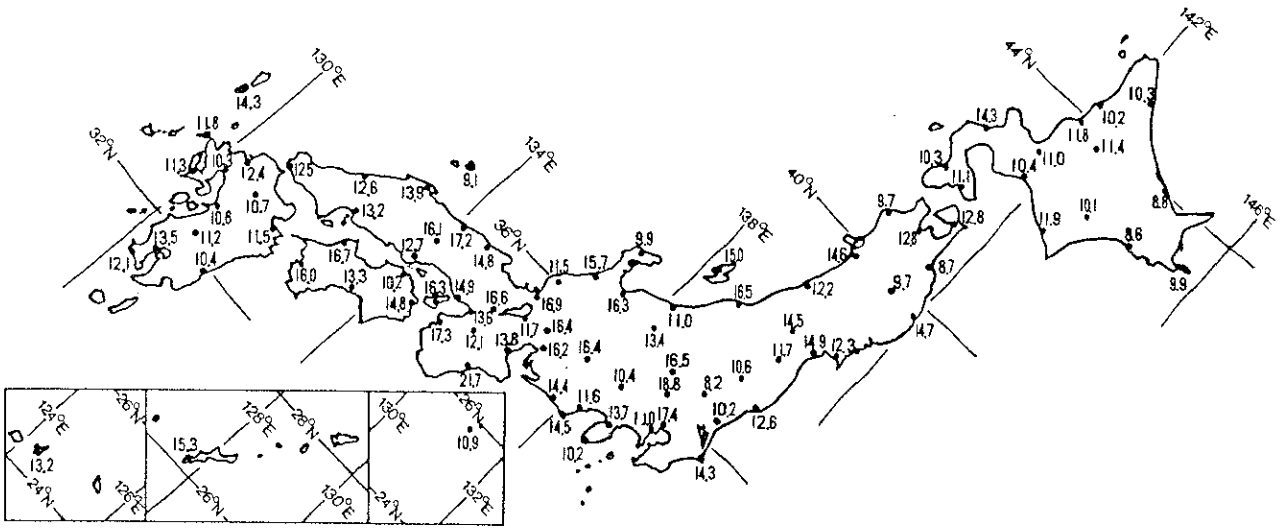

Figure 3 Distribution of the depth (m) to the isothermal layer in Japan.

is used here instead of the actual evapotranspiration. The heat flow by heat convection from the atmosphere into the ground is determined by the ground surface temperature and the recharge to the groundwater. The ground surface temperature in Japan varies at about the same period and phase in every region though the amplitude is different. In contrast, the recharge to the groundwater varies with different seasonal changes because the regional difference of seasonal changes in precipitation is large. Then, as a factor which indicates the seasonal deviation of recharge to the groundwater, Rs/Rw is shown in Figure 4, where Rs and Rw are the sums of recharge to the groundwater from May to October and from November to April, respectively. In this figure, the areas where Rs/Rw is small are located in Hokkaido and along the Sea of Japan, i.e., Tohoku, Hokuriku and San-in. In contrast, the areas where Rs/Rw is large are located in southern Kii Peninsula, southern Shikoku, central south of Kyushu and northern Kanto. Comparing Figure 2 with Figure 4, the areas where $T_{s3} - T_{s0}$ is large correspond to the areas where Rs/Rw is large.

Domenico and Palciauskas (1973) pointed out that the steady recharge concaves the temperature-depth profile. If this idea is applied to the seasonal change in the temperature-depth profile throughout the year, it is considered that the depth to the isothermal layer deepens with increasing steady recharge to the groundwater. However, the recharge to the groundwater varies seasonally. Therefore, when the monthly recharge to the groundwater is

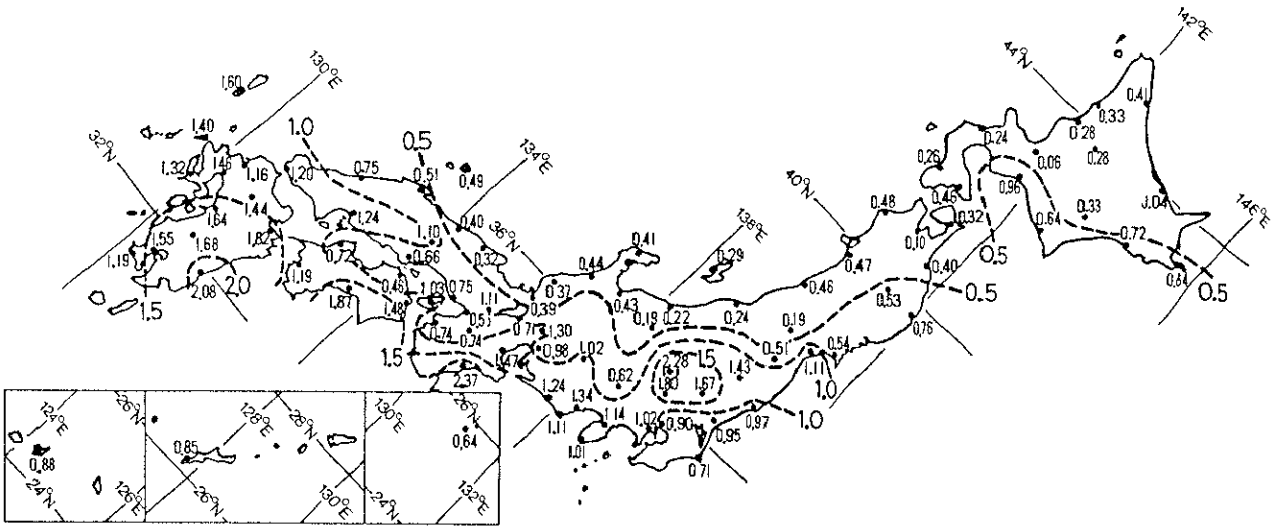

Figure 4 Distribution of Rs/Rw in Japan.
Rs : Recharge to the groundwater from May to October.
Rw : Recharge to the groundwater from November to April.

less than the mean of monthly recharge to the groundwater, it is assumed that the deviation is not available to deepen the depth to the isothermal layer. Distribution of the difference between the annual recharge to the groundwater (R) and the sum of the deviation (R*) in each point is shown in Figure 5. In this figure, the areas where R - R* is large are located along the side of Sea of Japan of Tohoku, Hokuriku and San-in, and Izu Peninsula, Atsumi Peninsula, southern Kii Peninsula, and southern Shikoku and Kyushu. In contrast, the areas where R - R* is small are located in eastern Hokkaido, the Pacific Ocean side of Tohoku and Seto-nai-kai. Though the areas where R - R* is large corresponds slightly to the areas where the depth to the isothermal layer is deep, the scatter of correspondence is large. Therefore, it is necessary to observe the detailed relationship between subsurface temperature and recharge to the groundwater in any area. In addition, it is necessary to clarify the relationship between the regional difference of subsurface temperature in any area and regional groundwater flow by which the difference is caused. This is because it is considered that subsurface temperature is affected not only by recharge but also by the other subsurface water flow.

In the following sections, the Nagaoka plain was selected as a study area to make clear the relationship between subsurface temperature and subsurface water flow, i.e., groundwater recharge, upward flow in the discharge area and other subsurface water movement. This is because the Nagaoka Plain is an area where the water cycle is very

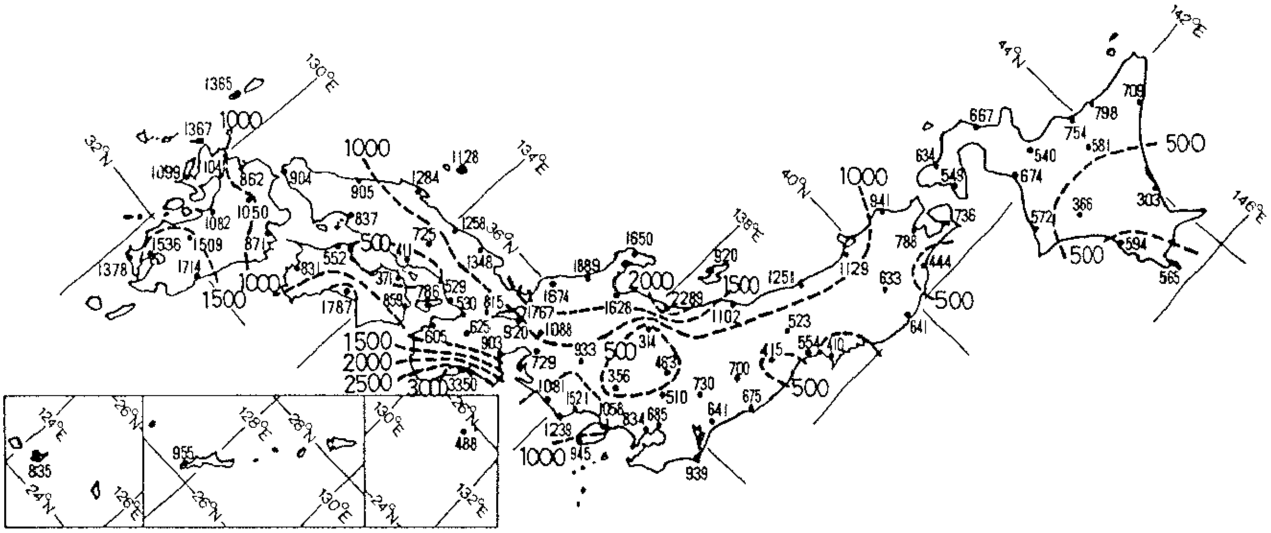

Figure 5 Distribution of R - R* (mm).
R : Annual recharge to the groundwater.
R*: Sum of deviation from annual mean of monthly recharge to the groundwater.

active. That means, it precipitates much as snowfall during winter in Nagaoka, and this area has a possibility of interaction between groundwater and river water due to adjacency to the Shinano River, and the groundwater level falls during winter due to pumping for melting snow accumulated on the roads (Tanaka et al., 1979; Kayane, 1980).

III. FIELD OBSERVATION OF SUBSURFACE TEMPERATURE IN NAGAOKA PLAIN

After showing the distribution of subsurface temperature and recharge to the groundwater temperature, it was indicated in Chapter 2 that the Nagaoka plain is selected as study area in order to clarify the relationship between the regional difference of groundwater temperature and the regional subsurface water flow by which the difference is caused. In this chapter, the explanations of the study area and the observation methods are shown in Section 3-1, and the thermal stabilities of water body in the wells and the aquifer are examined in Section 3-2 in order to confirm whether the water temperature measured in the wells represents the groundwater temperature at each depth.

3-1 Method

The explanations of the study area, instrumentation for measurements of hydrological and thermal conditions in the study area, and the observation method are shown in this section.

3-1-1 Study area

The study area, the Nagaoka plain, is in the south of the Niigata plain along the coast of the Sea of Japan,

Honshu, Japan (Figure 6). The main geological structure of the Nagaoka plain was formed by a series of crustal movements that occurred from the late Pliocene into the Pleistocene epochs. The surrounding hills are composed of thick sedimentary rocks of the Plio-Pleistocene period, which form the basement of the main aquifers in the plain.

According to bore hole records and aquifer test data, five main aquifers are distinguished in the groundwater basin. Mean hydraulic conductivities of these aquifers, identified as layers I, II, III and IV, are 0.120, 0.092, 0.022 and 0.018 cm/s, respectively in descending order (Nagaoka Construction Office, 1975). Columnar-sections along the lines a-a' and b-b' in Figure 6 are shown in Figure 7-a and Figure 7-b. The first and second aquifers are gravel-rich alluvial formations with a total thickness of about 20-40m, and the third and fourth are silt-contained formations. The surface of the plain is covered with a clayey layer (Figure 8). The northern part of the plain and the upper basin of the tributary have a thick clayey layer.

Figure 9 shows the seasonal change in monthly precipitation, evapotranspiration and air temperature in Nagaoka. The mean annual temperature and precipitation are 12.5 °C and 2654 mm/year, respectively. About 40 to 50 % of the precipitation falls as snow from November to March. This area is the first place where groundwater was used for snow melting. The annual evapotranspiration calculated by Penman's method is 707 mm/year. The actual evapotranspiration from vegetated surface was estimated from

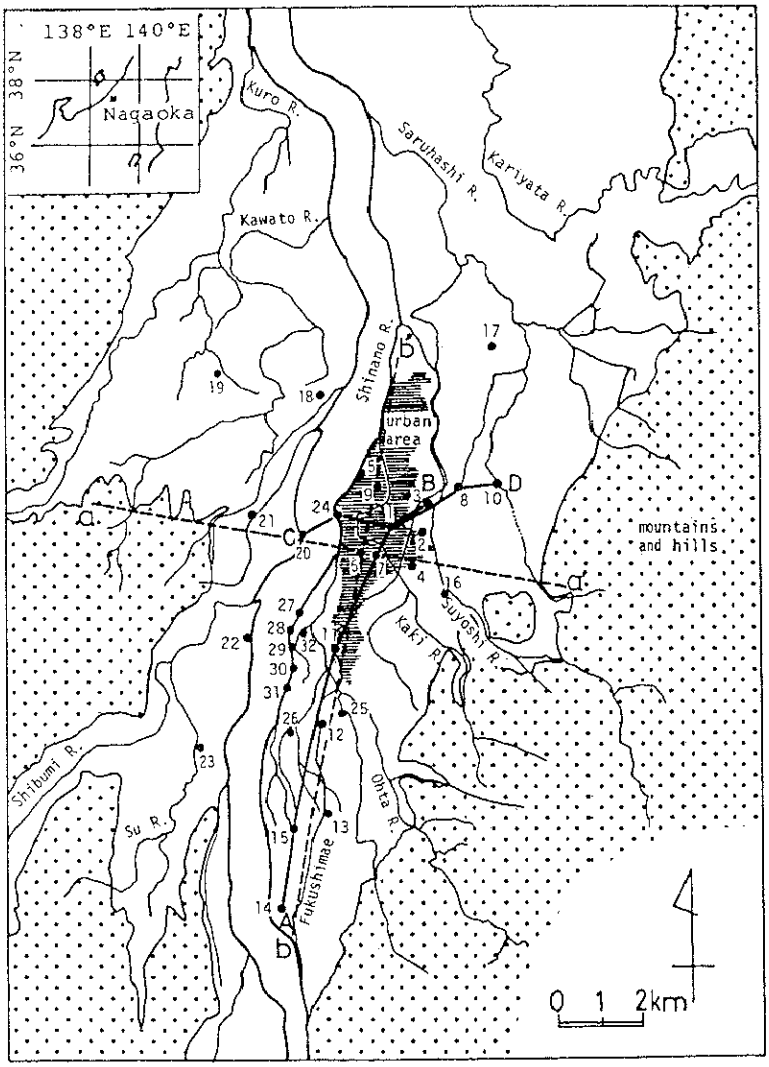

Figure 6 Study area and locations of observation wells.

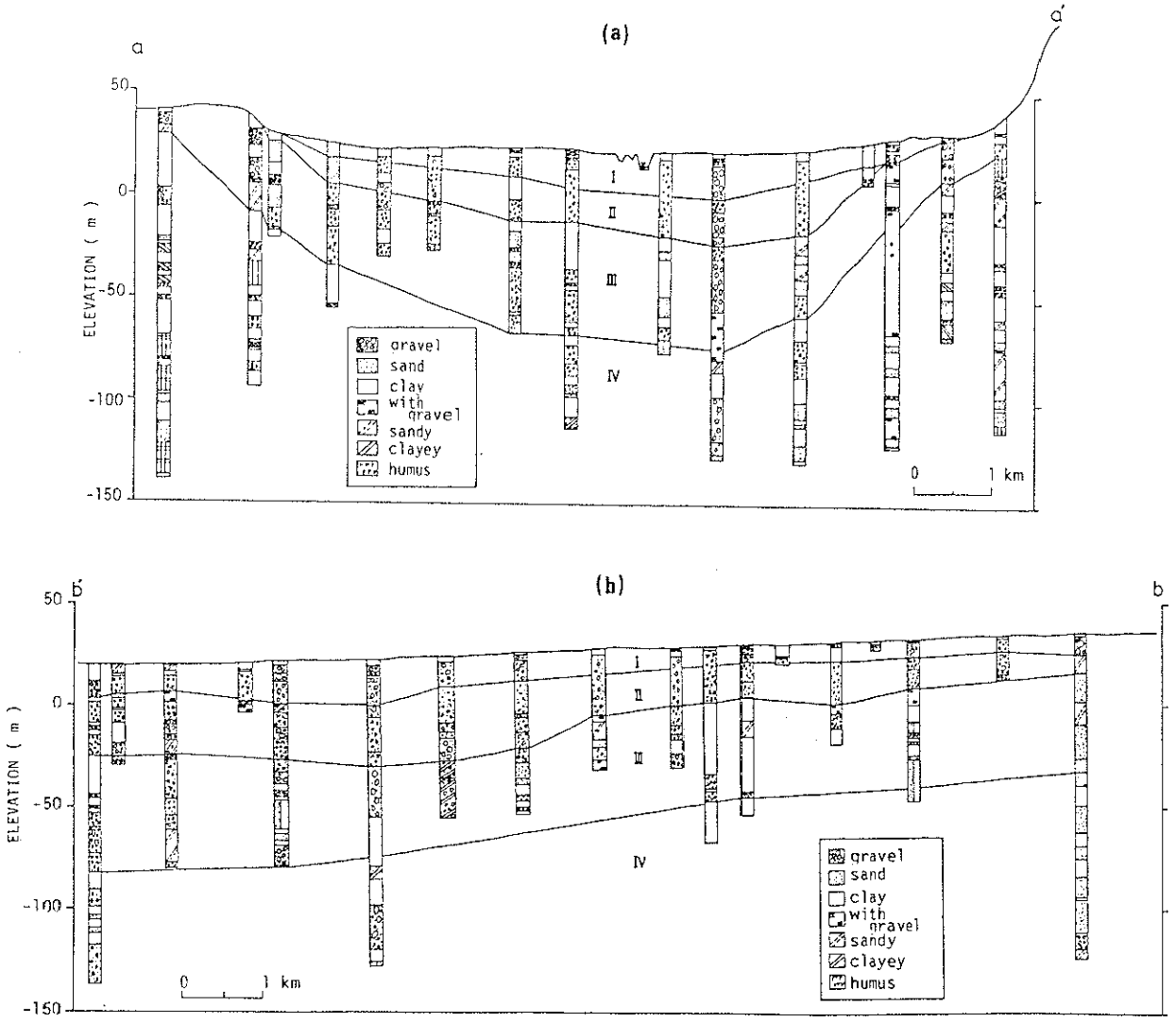

Figure 7 Columnar sections along (a) a-a' and (b) b-b' in Figure 6 (after Nagaoka Construction Office, 1975).

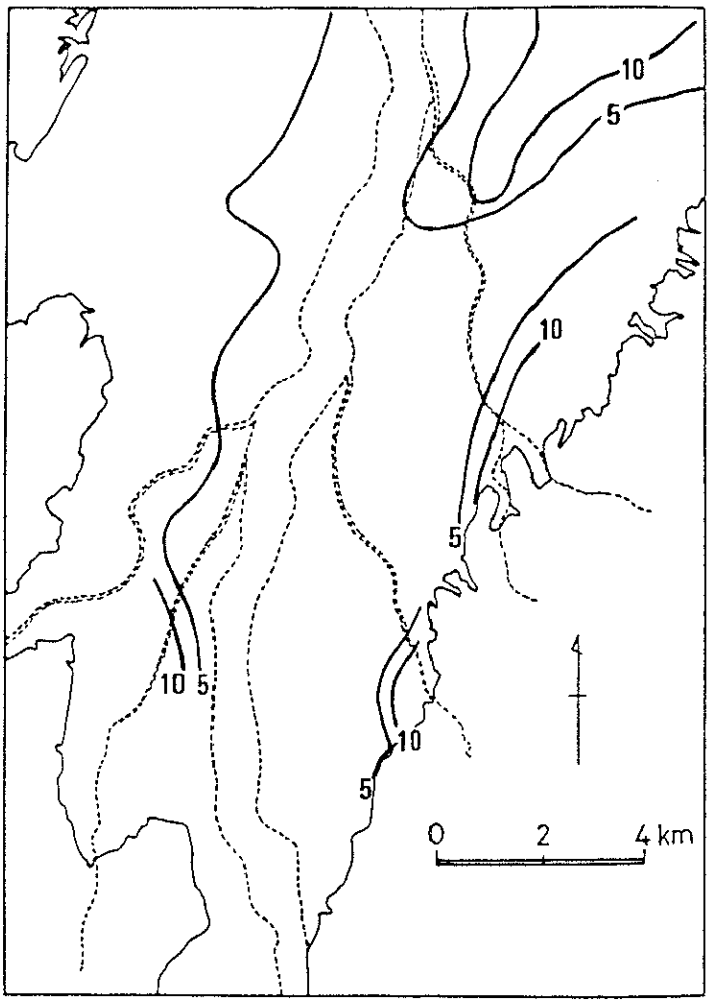

Figure 8 Contour map of the thickness of surface clayey layer (m).

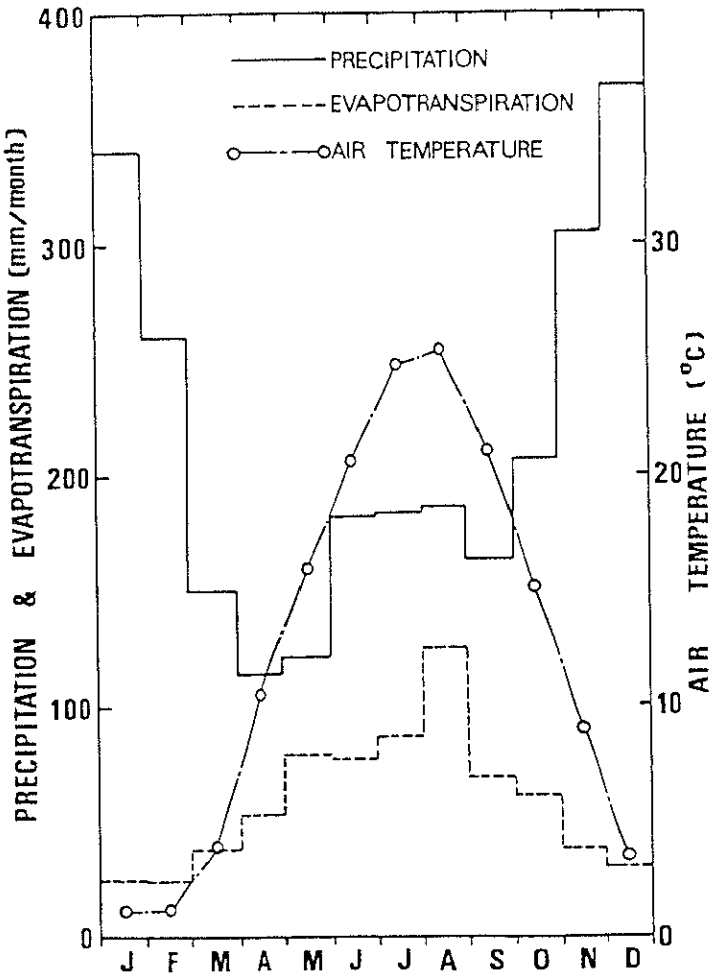

Figure 9 Seasonal changes in monthly precipitation, evapotranspiration and air temperature.

the potential evapotranspiration from the surface of the water by multiplying the Penman's empirical constant.

The Niigata Prefecture conducted a questionnaire survey on groundwater use in 1981 (Environmental Agency et al., 1982). The total number of wells in Nagaoka city was 12,895 and the annual amount of pumpage was 101,600,000 m^3/year in 259.9 km^2. Details of groundwater use are shown in Figure 10 by month and purpose. The groundwater use for snow melting occupies 80.5 % of the total pumpage for four winter months, and occupies 59.4 % of the annual pumpage.

3-1-2 Instrumentation

Soil temperature, thermal conductivity of soil and soil water content were measured in the unsaturated zone, and groundwater temperature and groundwater level were measured in 32 observation wells (Figure 6). The snow depth and the water equivalent of the snow cover were also measured at the point near the observation well W15 shown in Figure 6.

The soil temperature measured by a platinum resistance thermometer at depths of 4, 20, 40, 80, 120 and 170 cm below the surface, was automatically recorded from November 1982 to October 1983. The soil water content at the point near the observation well W15 was measured at one-week intervals during the snowmelt season in 1983 using the soil sampler at a depth interval of about 20 cm. The soil water content was obtained by the oven-dry method. The thermal conductivity of the soil at the point near the observation well W15 was

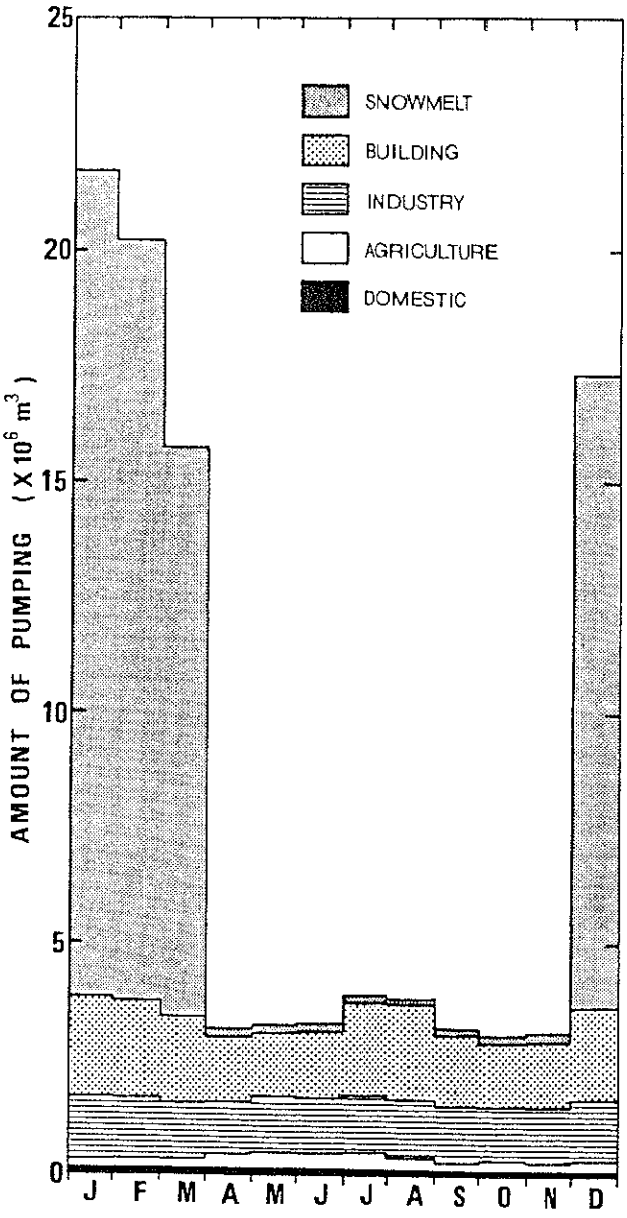

Figure 10 Seasonal change in monthly amount of groundwater pumping.

measured by using a conductivity meter at the depth of 80 cm below the surface. This instrumentation was devised based on so-called "probe method" (Taniguchi et al., 1982). In addition to this, the thermal conductivity was measured with a box probe of the quick thermal conductivity meter (Q.T.M.) using undisturbed soils in the laboratory in order to compare it with the data mentioned above.

The groundwater temperature was observed in 32 observation wells (Figure 6) using a thermistor thermometer which can read to 0.01 °C. Measurements were taken from the top to the bottom of the wells at two-month intervals from August in 1982 to August in 1983 and at four-month intervals from August in 1983 to August in 1985. In addition to this routine measurement, intensive measurements of groundwater temperature were made at one-week intervals during the snowmelt season in 1983 and from April in 1984 to March in 1985. The positions of the screen, the depths and the diameters of observation wells are shown in Table 1. The temperature field in the groundwater flow system can be detected by measuring the temperature-depth profile in the well if the temperatures within the water column of the well represent the temperatures of the fluid-porous medium complex adjacent to the wells. The relationship between the water temperature in the well and the groundwater temperature around the well will be described later in Section 3-2. The groundwater levels were measured continuously at observation wells using the automatic recorders provided by the Shinano-gawa Construction Office. In addition to this, the

Table 1 Depth, radius and the position of screen of the observation wells.

W	R (mm)	D (m)	S (m)	W	R (mm)	D (m)	S (m)
W1	100	22.0	14.0-22.0	W18	50	20.0	5.0-18.0
W2	100	50.0	28.0-44.5	W19	175	114.6	77.3-85.4
W3	100	22.0	11.0-22.0				96.6-99.5
W4	100	22.0	10.7-20.7	W20	50	20.0	5.0-18.0
W5	100	70.0	62.0-70.0	W21	50	20.0	4.0-14.0
W6	100	22.0	11.0-22.0	W22	50	20.0	5.0-18.0
W7	100	25.0	14.0-25.0	W23	50	20.0	3.0- 9.0
W8	100	25.0	14.0-23.0				13.0-18.0
W9	125	100.0	88.9-99.5	W24	75	20.0	7.0-17.0
W10	100	22.0	14.0-21.0	W25	100	96.0	64.0-70.5
W11	50	20.0	5.0-18.0				72.0-78.0
W12	50	20.0	5.0-18.0	W26	100	22.0	13.0-21.0
W13	75	76.0	51.5-60.0	W27	33	15.0	3.0-15.0
W14	50	20.0	5.0-18.0	W28	33	15.0	1.5-15.0
W15	50	20.0	5.0-18.0	W29	33	15.0	1.0-15.0
W16	75	85.5	67.0-77.5	W30	33	15.0	4.0-15.0
W17	175	97.5	68.4-77.4	W31	33	15.0	2.0-15.0
			82.0-85.0	W32	100	100.0	79.0-89.0
W17*	50	49.5	31.5-37.0				92.0-97.0
			42.0-49.5				

note) W:Well number, R:Radius, D:Depth, S:Screen

groundwater levels were measured at 30 shallow wells.

The snow depth was measured at six o'clock every morning by eye-measurement during the snow season from 1982 to 1983 and the snow density was also measured at one-week intervals during the snowmelt season in 1983. The snow samples were taken at a depth interval of 10 cm to measure the water equivalent of the snow cover.

3-2 Thermal stability of water bodies

Generally, heat is transported by both heat conduction and convection. Furthermore, heat convection is divided into free thermal convection and forced thermal convection. In this section, the effect of free thermal convection is calculated. Free thermal convection in the wells is examined in Section 3-2-1, then, free thermal convection in the aquifer is investigated in Section 3-2-2.

3-2-1 Free thermal convection in the wells

If the water temperature measured in a well at any depth is the same as the groundwater temperature around the well, it becomes very easy to investigate the groundwater temperature distribution in space and time. For that reason, it is necessary to check the thermal stability of the water column in a well.

Problems encountered in obtaining representative groundwater temperatures from wells have been discussed by

many authors (e.g. Boyle and Saleem, 1979). Krige (1939) developed an expression for the critical gradient Gc of a fluid-filled column as follows:

$$Gc = \frac{gaT}{c_0} + \frac{C\nu\alpha}{gar^4} \qquad \text{.....(6)}$$

where

g = acceleration due to gravity;

T = absolute temperature;

a = volume coefficient of thermal expansion of the fluid;

c_0 = specific heat of the fluid;

α = thermal diffusivity of the fluid;

ν = kinematic viscosity of the fluid;

r = radius of the column;

C = a constant, equal to 216 in cgs units.

The critical gradient Gc is defined in equation (6) as the temperature gradient when the convective flow is incipient. A situation in which the temperature increases with the depth will be thermally unstable when the actual temperature gradient exceeds the critical gradient.

In this study, the radii of observation wells were from 3.25 to 12.5 cm, most of them being 5 or 10 cm (Table 1). The critical gradient Gc was calculated using equation (6) with the following values : g = 980 cm/s^2 , T = 285.8 K, a = 2.18×10^{-5} /°C, c = 4.19×10^7 ergs/g·°C, $\nu = 1.002 \times 10^2$ cm^2/s $\alpha = 1.4 \times 10^{-3}$ cm^2/s, C = 216 and r = 5 or 10 cm. The calculated Gc of 2.27×10^{-2} °C/m for r = 5 cm and 1.42×10^{-3}

°C/m for r = 10 cm were exceeded by the actual temperature gradients of the March, April and June profiles for most wells.

Then, in order to examine whether the free convection practically occurs in the well, the author compared the actual temperature gradient with the critical gradient in the two wells having different Gcs with the different radius at the same point where the observation well W17 is located. Figure 11 shows the difference of groundwater temperatures in two wells whose radii are 10 cm and 5 cm. In this figure, the bars show the periods when the actual temperature gradient does not exceed the critical gradient. If the theory of the critical gradient is applicable, the difference in groundwater temperature should be large during November and December when the critical gradient is exceeded in the larger well (W17) and not exceeded in the smaller one (W17*). However, the difference in groundwater temperature is small throughout the year. This may be due to frictional resistance at the wall of the well and so on. Therefore, it may be concluded that the water temperature measured in a well at any depth is representative of the groundwater temperature at the same depth around the well.

3-2-2 Free thermal convection in the aquifer

Vertical water flux in the aquifer caused by the free thermal convection under the assumption that groundwater flows horizontally as a piston flow, is shown as follows

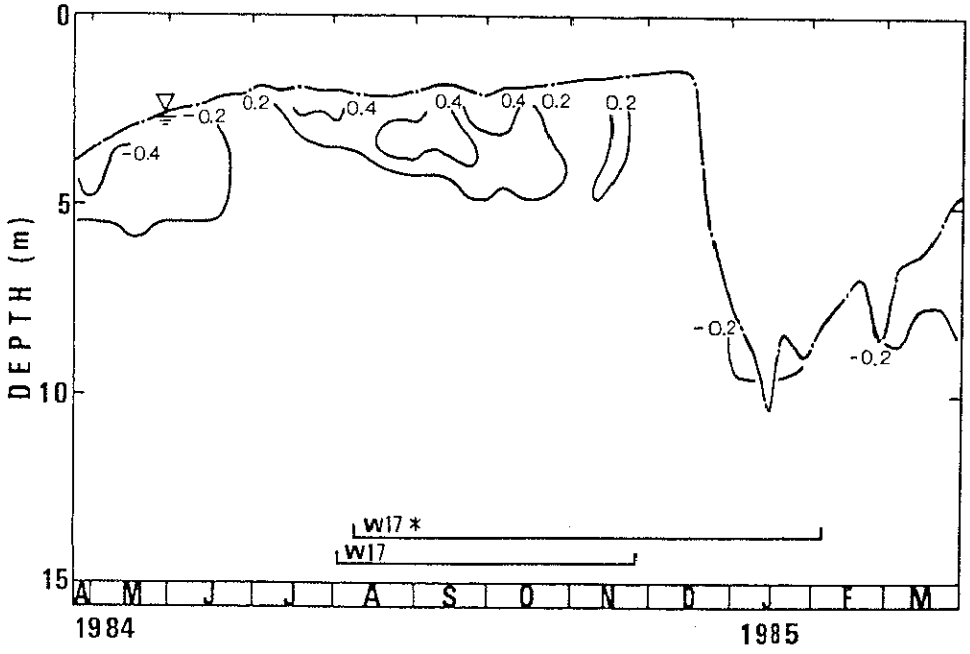

Figure 11 Difference of water temperature (°C) between wells W17 and W17*, and the period when the actual temperature gradient does not exceed the critical gradient.

(Claesson, 1978):

$$|qz| = \frac{Kz}{Kx} \cdot \frac{Kx(Tc)}{1 + N} \cdot \frac{\gamma c - \gamma h}{\gamma c} \qquad \text{.....(7)}$$

where

|qz| = water flux in vertical direction by free thermal convection

Kx = hydraulic conductivity in x direction

Kz = hydraulic conductivity in z direction

Tc = temperature of cold water

γc = specific gravity of cold water

γh = specific gravity of hot water

N = ratio of coefficient of viscosity

If it is assumed that the lowest water temperature (Tc) and the highest one (Th) in the aquifer are 0 °C and 30 °C, respectively, the ratio of the coefficient of viscosity N = $\mu(30°C)/\mu(0°C)$ is equal to 0.45. Generally, Kz/Kx ranges from about 10^{-1} to 10^{-2} and Kx(0 °C) = Kx(20°C) x μ(20 °C)/μ(0 °C) (Bouwer,1978). Therefore, the vertical flux caused by the free thermal convection was calculated using equation (7) and the following values: γ(0 °C) = 0.9998, γ(30 °C) = 0.9957, μ(0 °C) = 1.792×10^{-2}, μ(20 °C) = 1.002×10^{-2}, μ(30 °C) = 0.797×10^{-2} Pa·s, Kx(20 °C) = 1.2×10^{-3} m/s.

As a result, |qz| was obtained as 1.25×10^{-7} m/s (= 3.95 m/year). However, this flux indicates the value under the condition that the boundary of hot and cool water bodies exists throughout the year. Therefore, the vertical flux in

the aquifer caused by the free convection is smaller than the calculated value in fact, and it may be neglected in this study.

IV. CHANGES IN SUBSURFACE TEMPERATURE IN TIME AND SPACE

The results of measurements and qualitative explanations of subsurface temperatures in the study area are shown in this chapter. Seasonal changes in soil and groundwater temperatures are indicated in Sections 4-1 and 4-2, respectively. The results of observations of subsurface temperature to hydrological events and secular variations of subsurface temperature are shown in Sections 4-3 and 4-4, respectively.

4-1 Seasonal variation of soil temperature

Figure 12 shows the seasonal variations in the daily mean of soil temperatures at the depths of 4, 20, 40, 80, 120 and 170 cm below the surface, from November 1982 to October 1983, at the point near the observation well W15 shown in Figure 6. Blanks in Figure 12 show the periods when there was insufficient measurement.

The air temperature in the study area changed sinusoidally with the highest and lowest temperatures in the first part of August and February, respectively. When the air temperature changes sinusoidally, the soil temperature also changes in the same way. However, the phase of soil temperatures delays, and the amplitude decreases with the increasing depth.

When the air temperature increases from spring to summer

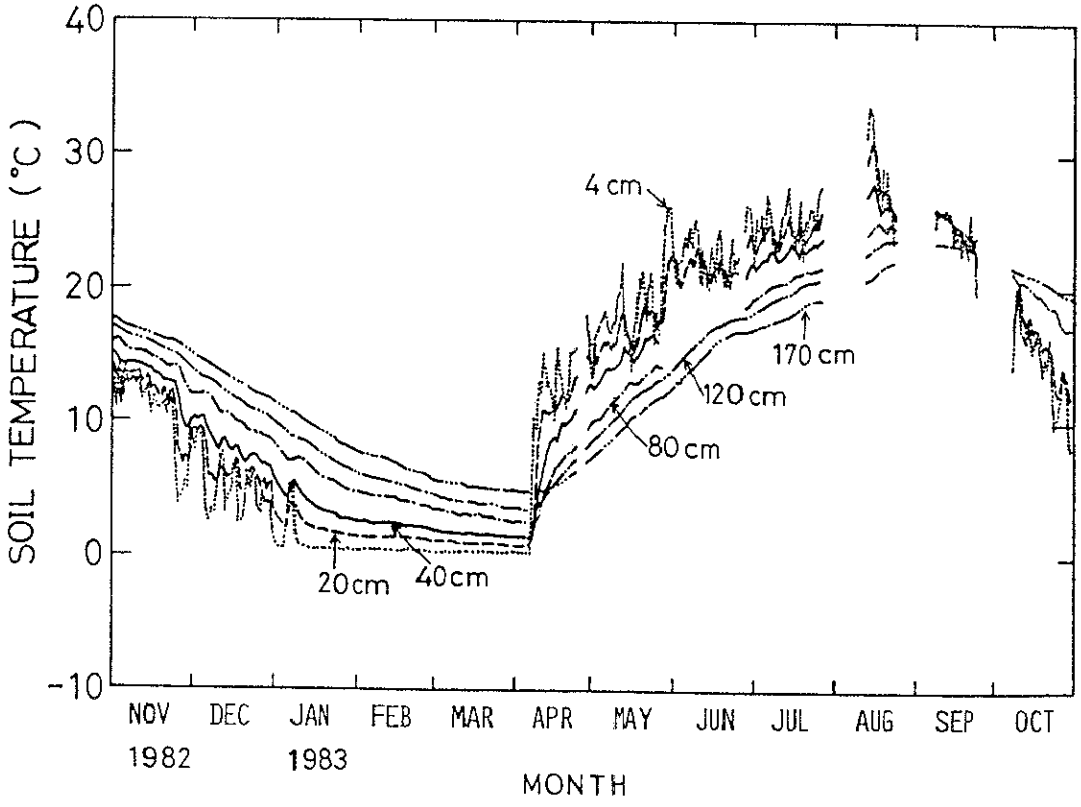

Figure 12 Seasonal variation of soil temperature at each depth at the point near the well W15.

in Nagaoka, the soil temperature changes as mentioned above. That is to say, the soil temperature at each depth increases from the middle of April to the beginning of August, and temperature of the deeper soil is higher than that of the shallow layer. After August, the deeper the depth below the surface is, the later the time of the highest soil temperature at each depth is. The gradient of the soil temperature disappears from the ground surface to a depth of 170 cm in the middle of September.

Accordingly, when the air temperature decreases from autumn to winter in Nagaoka, the soil temperature changes characteristically. After the beginning of January, the soil temperature of the ground surface is maintained at 0 °C on account of the snow cover. Even though the air temperature starts to increase after the first part of February, the temperature of the ground surface remains at about 0 °C and the soil temperature at each depth decreases. As soon as the snow cover disappears at the first of April, the soil temperature of the surface increases rapidly and the gradient of the soil temperature profile is reversed successively from the surface. After the middle of April, the temperature of the soil decreases from the ground surface to a depth of 170 cm.

4-2 Seasonal variation of groundwater temperature

Though seasonal variations of the subsurface temperature in the unsaturated zone were indicated in Section 4-1,

seasonal variations of subsurface temperature in the saturated zone are shown in this section. Seasonal changes in horizontal and vertical two-dimensional distributions of groundwater temperature are indicated in Sections 4-2-1 and 4-2-2, respectively. In addition, the classification of temperature-depth profiles are made in Section 4-2-3.

4-2-1 Horizontal two-dimensional distributions

Figures 13-a to 13-f show water table contours in meters above sea level. The Shinano River is naturally a gaining stream fed from groundwater all through the reach in the study area, as shown in the August and October water tables of Figures 13-f and 13-a. During the winter, the water table at the center of the city drops to a level lower than the water level of the Shinano River owing to heavy pumping of groundwater used for snow melting (Figure 13-c). The decline of the water table induces artificial seepage from the river into the groundwater (Kayane et al., 1985). The recovery of the water table is very rapid in April (Figure 13-e).

Figure 14 shows the seasonal changes in the isothermal lines of the groundwater temperature at depths of 5, 10 and 15 m. Since the normal groundwater temperature at the depth of 20 m below the surface is about 12-13 °C, the regional differences in the shallow groundwater temperature shown in Figure 14 are strongly influenced by recharge into or discharge from the groundwater body, by induced water from the river due to pumping and by the movement of the

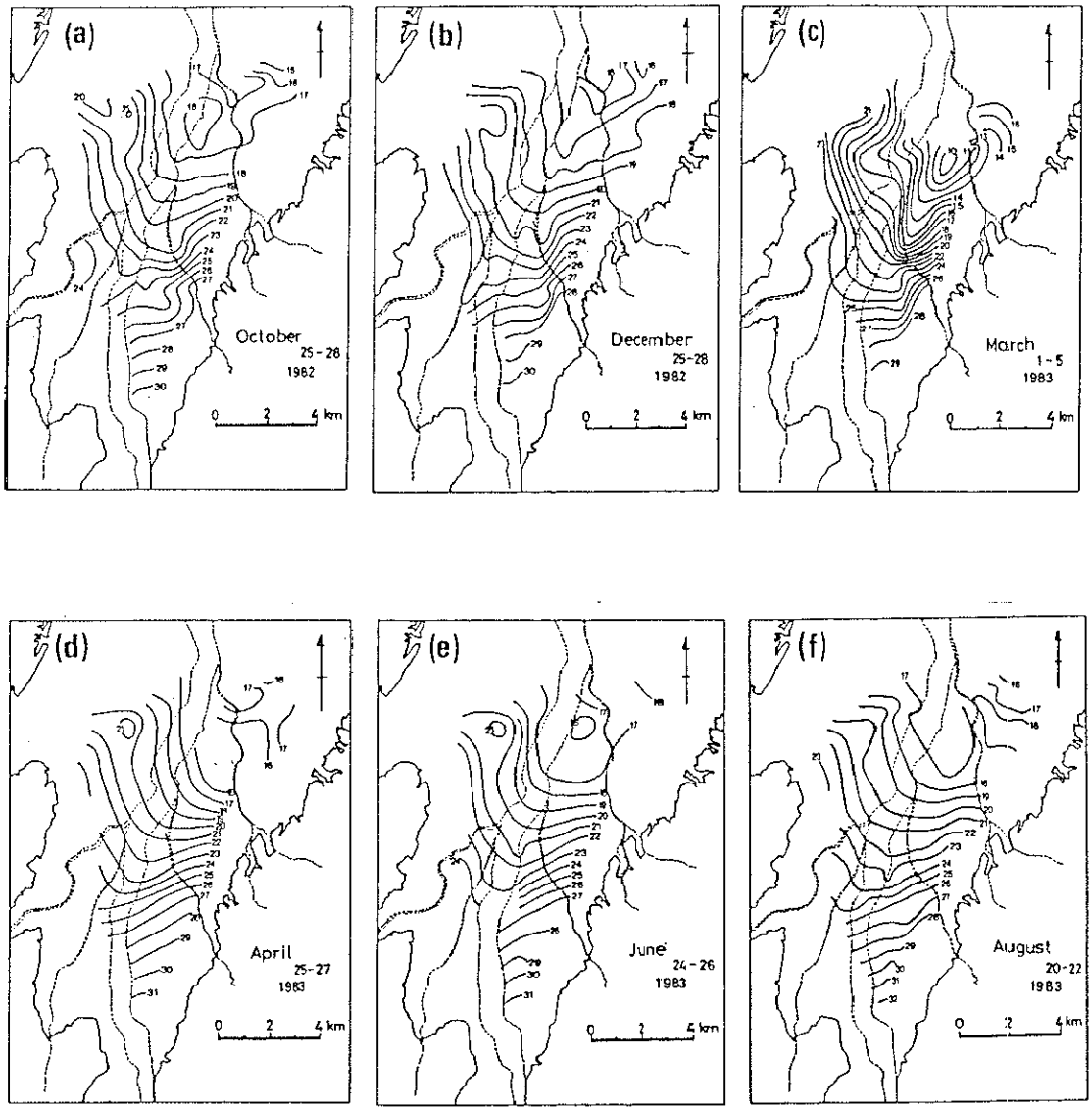

Figure 13 Seasonal change in contour map of the water table (meter above sea level).

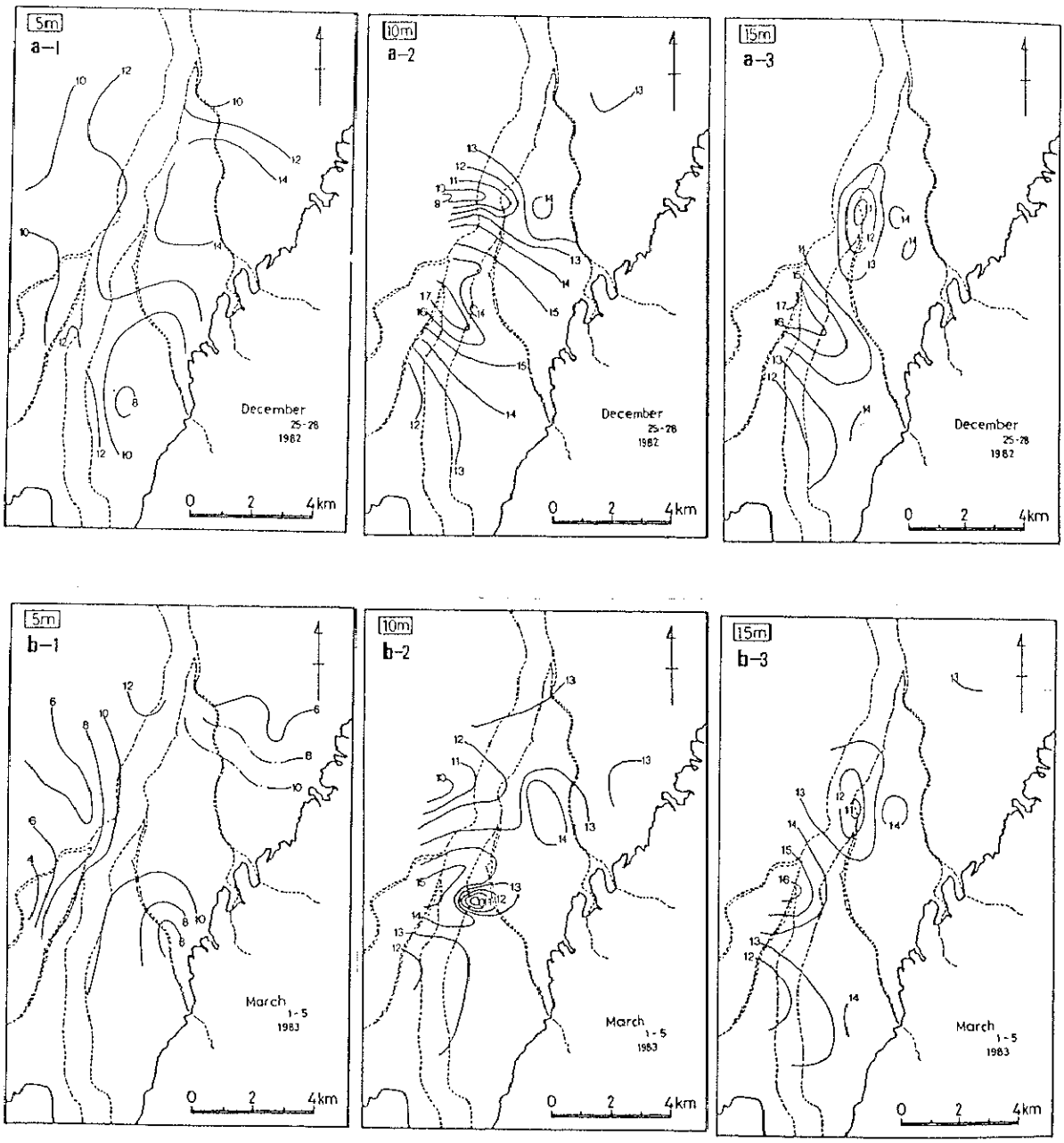

Figure 14 Seasonal change in horizontal two-dimensional distributions of groundwater temperature (°C) at the depths of 5, 10 and 15 m.

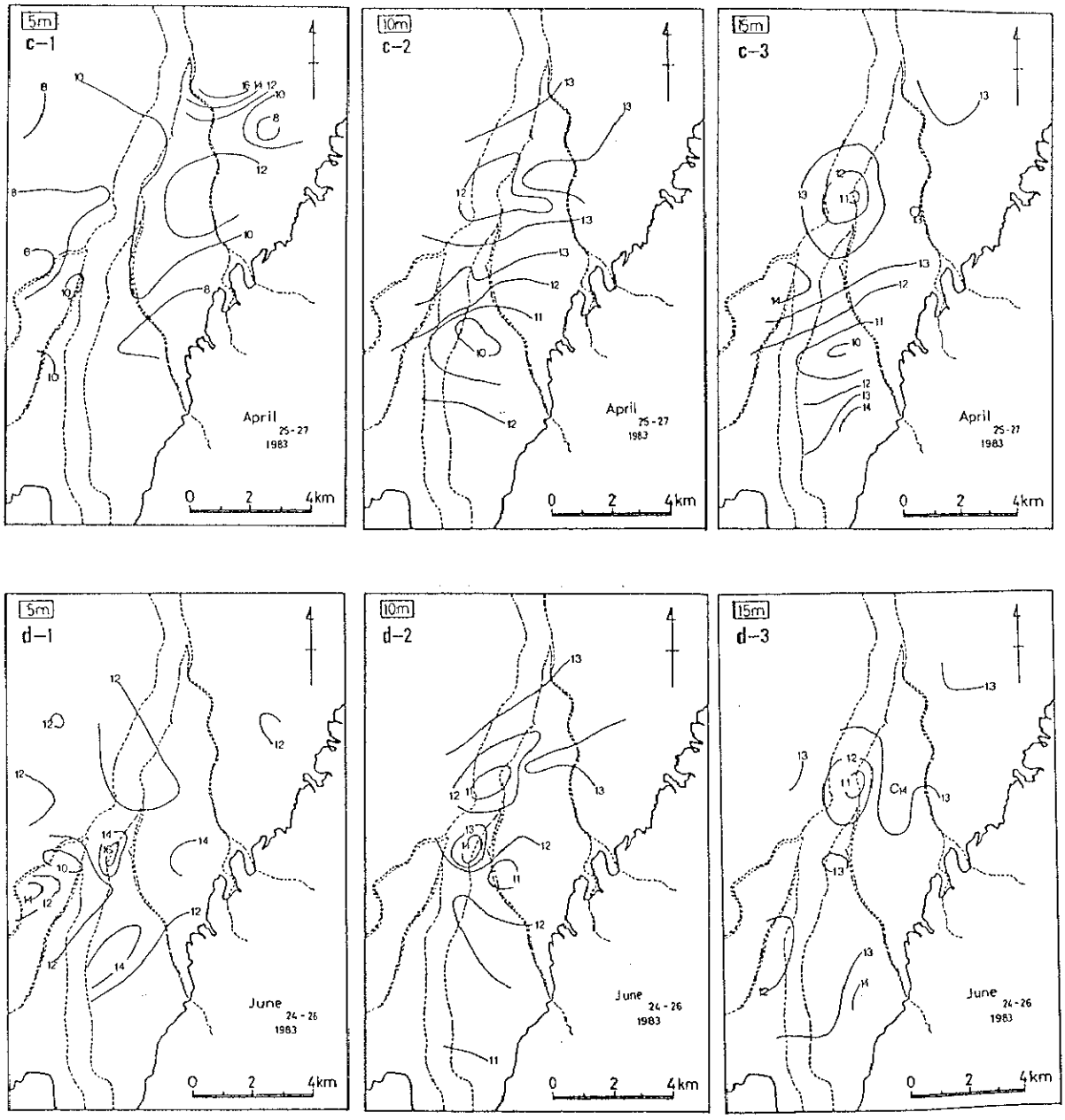

Figure 14 (continued)

groundwater itself.

In December at 5 m depth (Figure 14-a-1), warm groundwater zones higher than 14 °C are found in the urban area, and lower than 10 °C are found to the south of the Ohta River and upstream of the Shibumi River. In June at the 5 m depth (Figure 14-d-1), warm groundwater zones located in the south and cold groundwater zones are found in the north area in contrast with December. From the isoplethes at depths of 5 m and 10 m, it can be seen that the effects of tributary water on the groundwater is marked at the shallow layer.

From December to March at the 10 m depth (Figures 14-a-2 and 14-b-2), the warm groundwater zone expands in the urban area, though the groundwater temperatures decrease in other areas. This is caused by the downward movement of the warm groundwater zone which is found in the shallow layer before winter, induced by pumping of groundwater from the deep layer. In March and April at the 10 m depth (Figures 14-b-2 and 14-c-2), the induced recharge of cold water from the Shinano River to groundwater is recognized in the urban area owing to the lowered water table due to pumping.

From the isothermal lines at the depth of 15 m, it is supposed that a negative heat source is located in the west of the urban area under the Shinano River and that a heat source is located near the foot of the east mountain throughout the year.

4-2-2 Vertical two-dimensional distributions

The distributions of groundwater temperatures in the vertical two-dimensional domain are presented in this section. Figure 15 shows seasonal changes of the groundwater temperature distribution in vertical cross sections along lines A-B and C-D in Figure 6. Since the seasonal changes in groundwater temperatures are repeated year by year in a more or less similar manner, it is easier to understand Figure 15 if the author begins the explanation with the August patterns. In August, the vertical advective effect by percolation of warm irrigation water occurs first in W14 and W15 in the south area, and the horizontal advective effect from the Shinano River is recognized in the C-D cross section. Then in October, a warm groundwater layer higher than 14 °C is formed immediately below the water table, and the thickness of the layer increases with time until December. The water temperature in the Shinano River is lower than that of groundwater in October, but its effect is not recognized in the October pattern. The water table drops in winter on account of extraction of groundwater through wells, and then it starts recovering in March. Cold layers lower than 12 °C first occur in W14, W15, W20 and W24 near the Shinano River in March. The thickness and extent of the cold layer grow with time until June when the warm layer starts appearing in W15. The influence of the cold induced water from the Shinano River due to pumping is conspicuous in April in the C-D cross section. A warm groundwater body higher than 14 °C found throughout the year in W1 seems to be an indication of an upward flow of warm groundwater due to

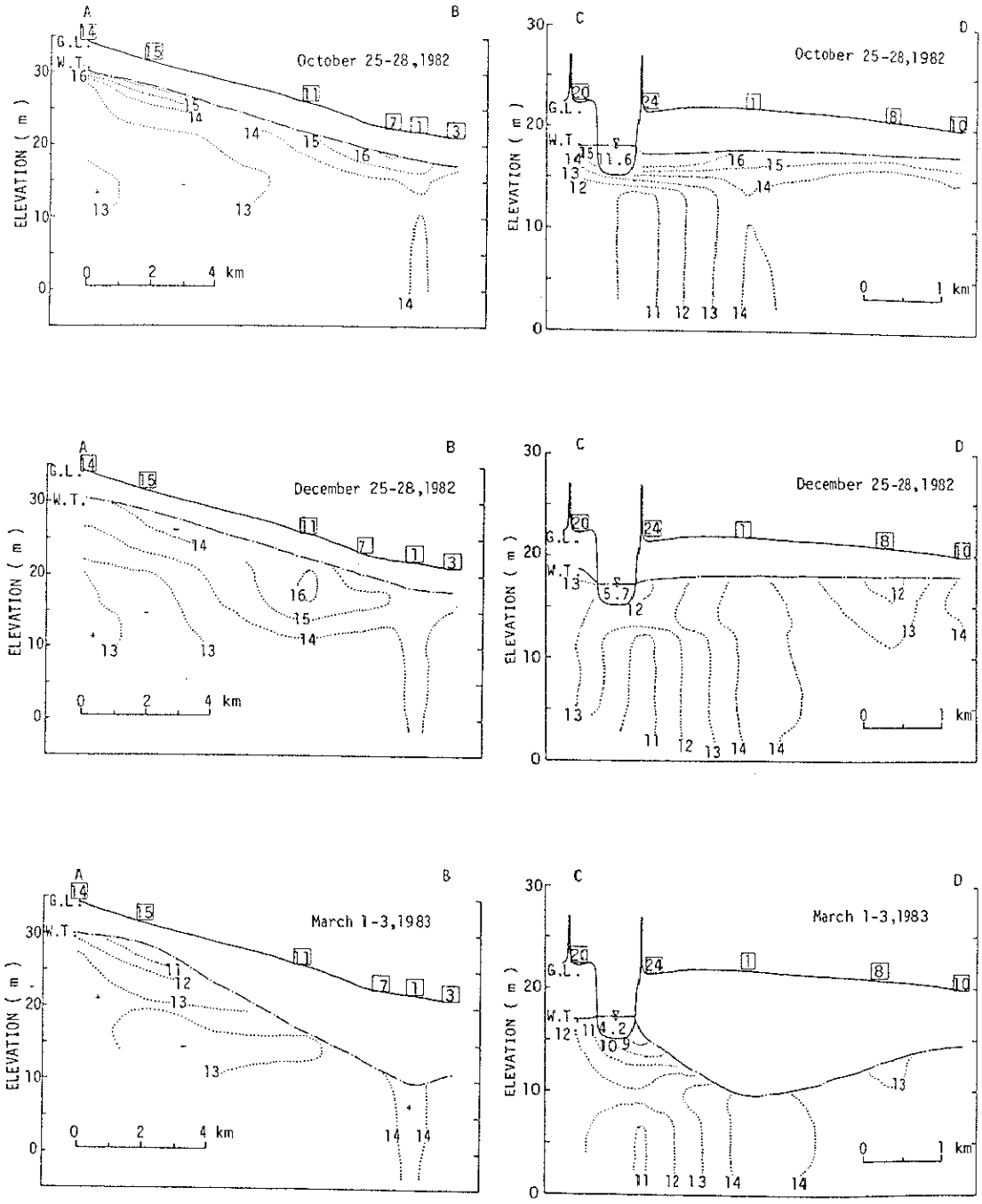

Figure 15 Seasonal changes in groundwater temperature (°C) along A-B and C-D in Figure 6.

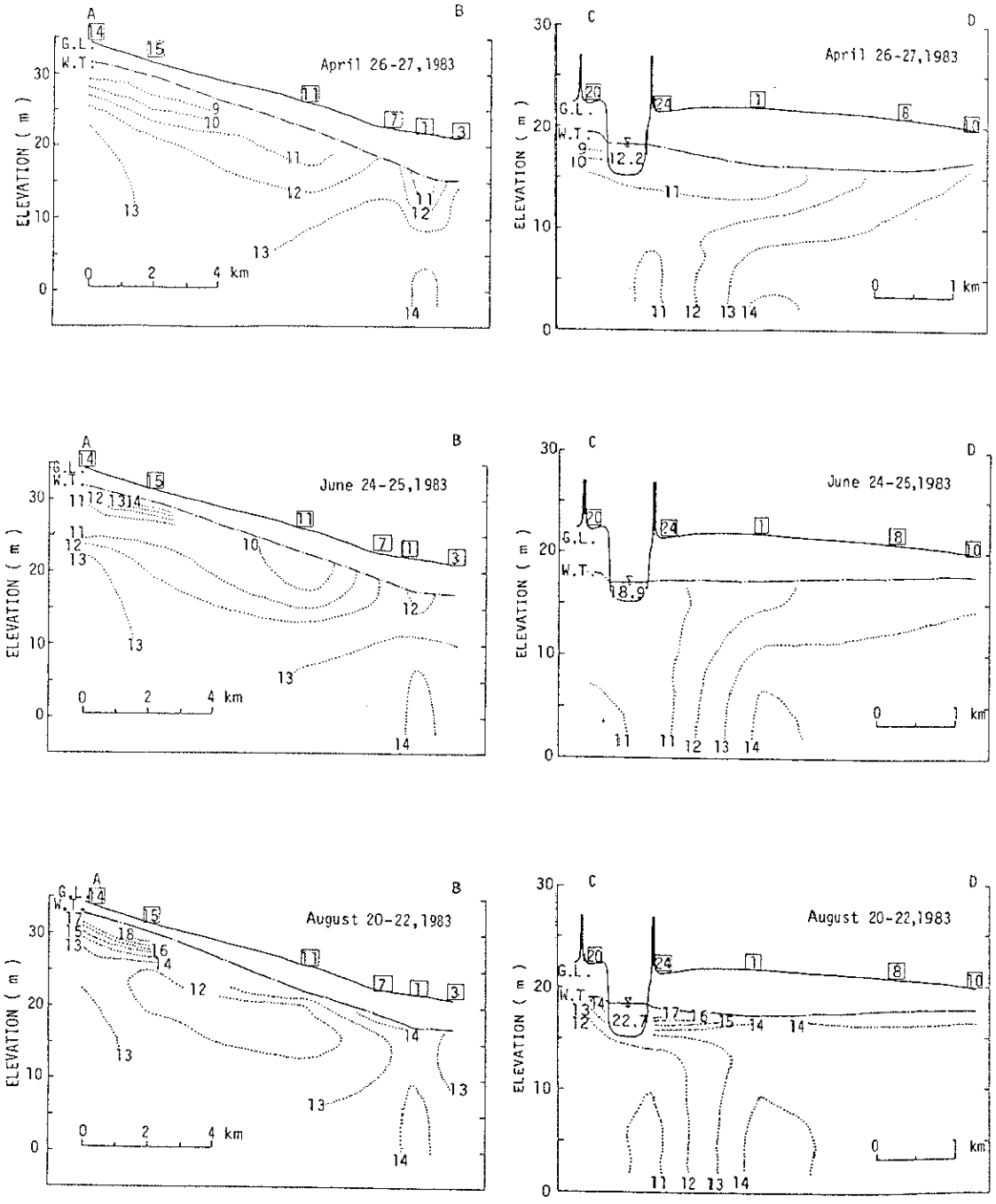

Figure 15 (continued)

pumping, because a positive heat source exists below the sea level.

4-2-3 Temperature-depth profiles

The temperature-depth profiles in 32 observation wells are classified into the following four types according to the pattern of seasonal variation. As typical examples of the four types, observed temperature-depth profiles and time-depth variations of groundwater temperatures in the wells W15, W18, W31 and W6 are shown in Figure 16 and Figure 17, respectively. The profiles of the other wells are indicated in Figure 18. The circled numbers in Figure 18 indicate the number of the observation wells.

Typical temperature-depth profiles and time-depth variations of groundwater temperatures of the A type are shown for W15 in Figures 16-a and 17-a. The location of this well is near the head of the alluvial fan where the aquifer is gravel-rich and its hydraulic conductivity is high. Features of the A type to be noted are undisturbed but vertically elongated temperature-depth profiles, and the larger depth to the isothermal layer which is 18 m below the surface. Generally speaking, the depth to the isothermal layer in Japan is from 12 m to 14 m, excepting Hokkaido. The mean subsurface temperature is higher by 1 to 2 °C than the mean air temperature (equation (4)). For that reason, the mean subsurface temperature in Nagaoka Plain should be from 13 to 14 °C. However, the temperature-depth profiles of A type

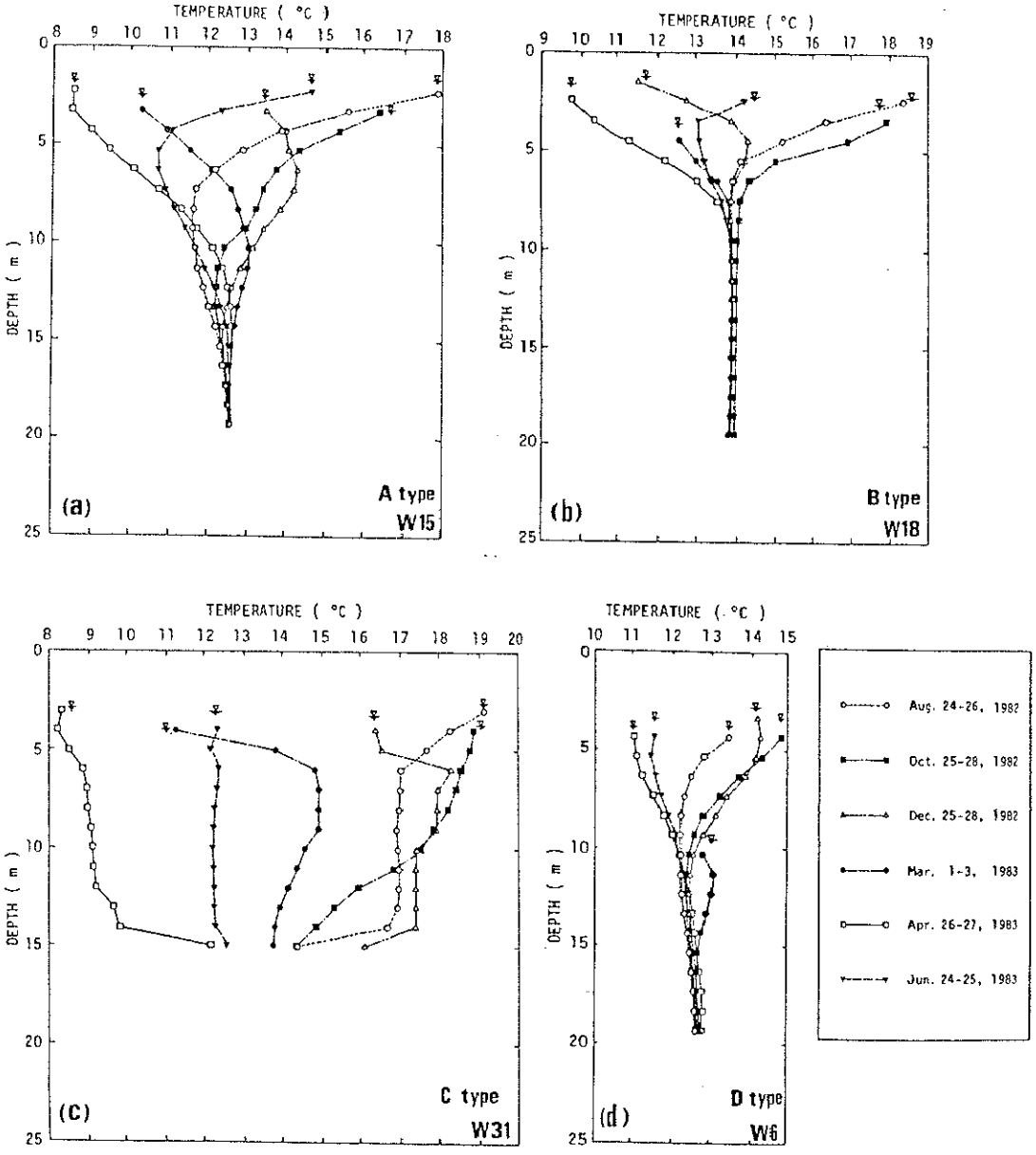

Figure 16 Temperature-depth profiles in four typical wells.

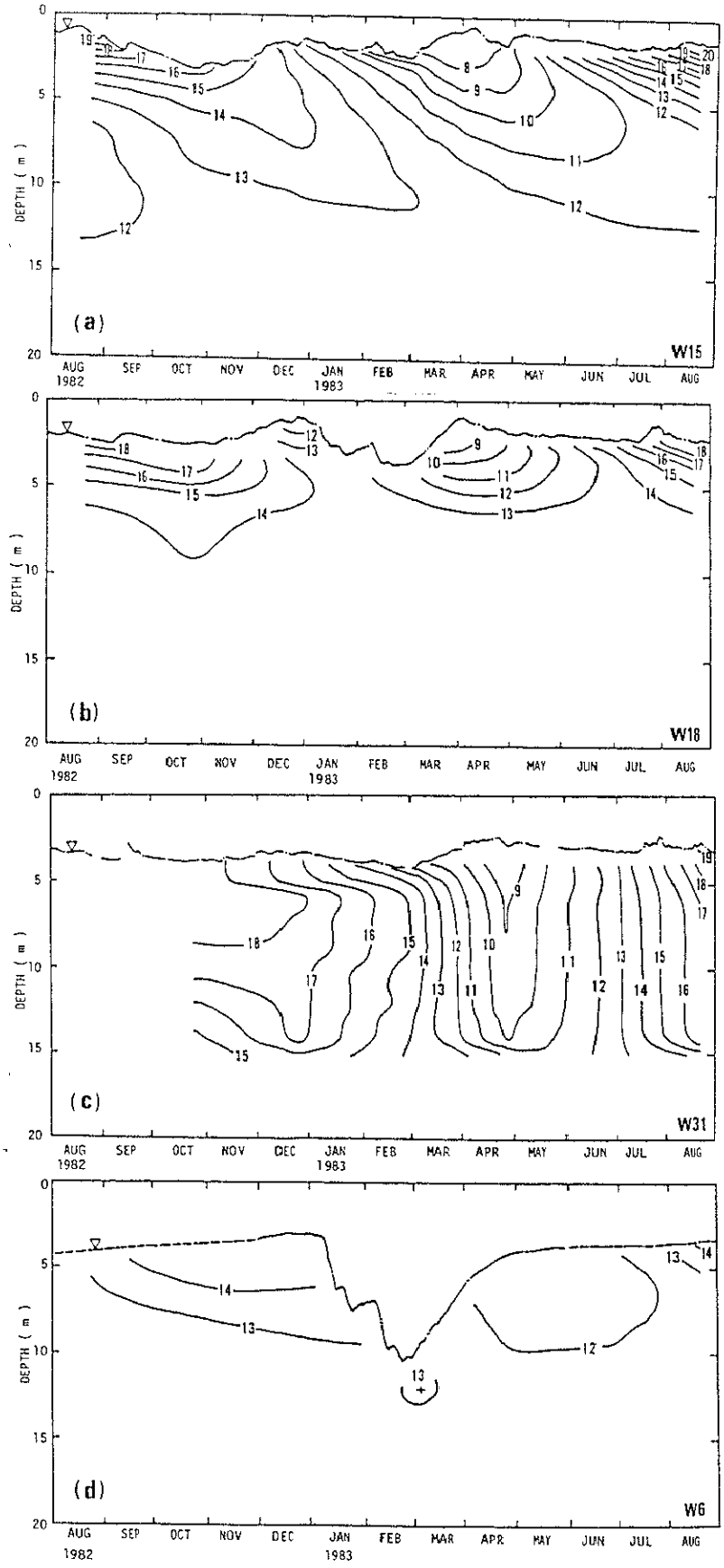

Figure 17 Time-depth variations of groundwater temperature (°C) in four typical wells.

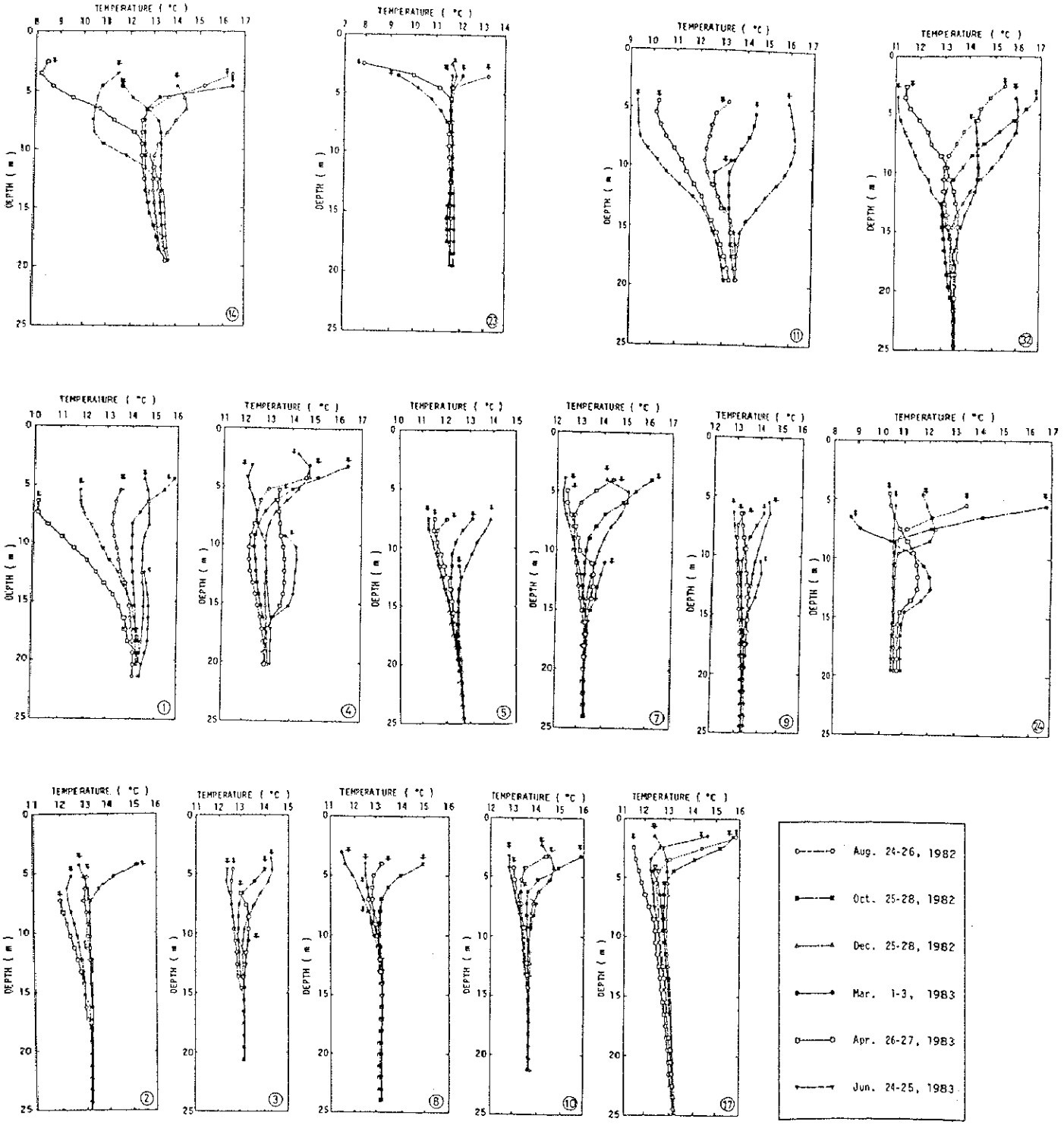

Figure 18 Temperature-depth profiles in observation wells.

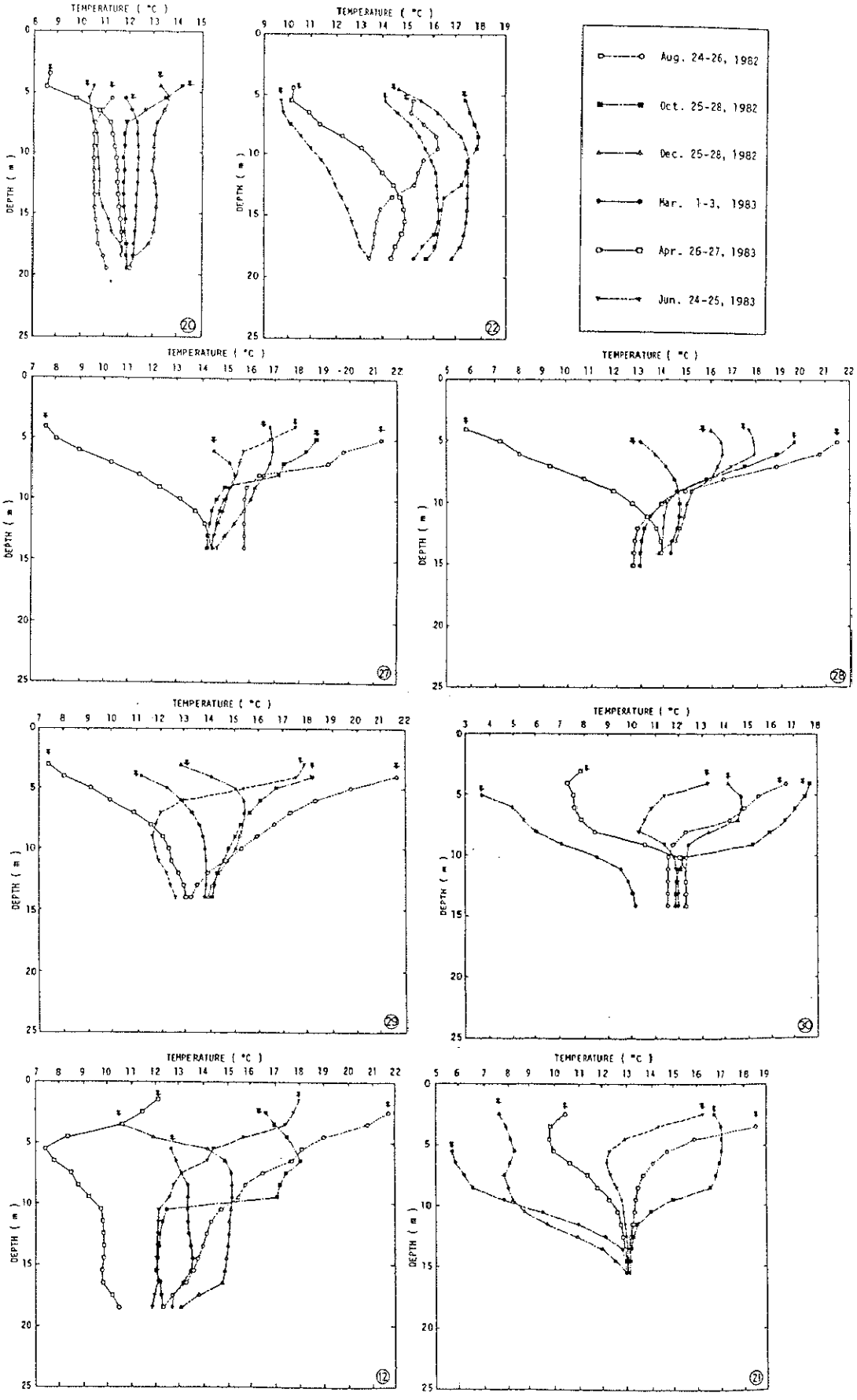

Figure 18 (continued)

shift to low temperature. The profile for W14 (Figure 18) may also be classified as of the A type, but shifts to low temperature in June and October, and shifts to high temperature in August in the layer at the 5-10 m depth.

Typical temperature-depth profiles and time-depth variations of groundwater temperatures of the B type are shown for W18 in Figures 16-b and 17-b. The well is located near the Shinano River in a constant groundwater discharging zone throughout the year as can be seen in Figure 13. Features of the B type profiles are undisturbed but vertically compressed temperature-depth profiles, and the smaller depth to the isothermal layer which is about 13 m below the surface. The temperature-depth profiles of the B type shift to higher temperature than A type well. The temperature-depth profile for W23 (Figure 18) is similar to the B type in the view that the depth to the isothermal layer is small. However, the base groundwater temperature which does not change throughout the year in the deep layer, of 13.8 °C in W18 is higher and that of 11.6 °C in W23 is lower than the normal groundwater temperature of 12.7 °C which is equal to the mean annual air temperature for 10 years in Nagaoka.

Typical temperature-depth profiles and time-depth variations of groundwater temperatures of the C type are shown for W31 in Figures 16-c and 17-c. Nine wells are classified as of the C type, but they may be divided further into three groups according to their locations relative to rivers feeding the water to groundwater; the left bank group

(W20 and W22), the right bank group (W27, W28, W29, W30 and W31), and the canal or tributary group (W12 and W21). Generally speaking, the Shinano River is a gaining stream in the study area, so that the direction of the groundwater flow is to the Shinano (Figure 13). This means that the flow of groundwater along the Shinano has its west component on the left bank and its east component on the right bank. An exception is found in the zone where wells W27 to W31 are located. In this zone, the seepage from the Shinano to groundwater is predominant because the zone coincides with an old channel of the Shinano found in historical maps (Kayane, 1980). Therefore, the advective effect of the Shinano is stronger in wells of the right bank group than in those of the left bank group and resulted in larger annual amplitudes of groundwater temperature for the right bank group than for those of the left bank group. Though wells W12 and W21 are distant from the Shinano, a big irrigation canal named Fukushimae and a tributary run near the wells W12 and W21. The influence of advected water on temperature-depth profiles is exclusively controlled by hydrogeological conditions. Marked irregularities in the local hydrogeology are reflected in the patterns of temperature-depth profiles for wells W28, W30 and W31.

Typical temperature-depth profiles and time-depth variations of groundwater temperatures of the D Type are indicated for W6 in Figures 16-d and 17-d. The D type wells are located in the center of the city where a large "cone of depression" is formed due to the areal effect of groundwater

pumping for snow melting. The most interesting feature of this type is the formation of a warm layer at the 10-15 m depth in March except for well W1 in which the depth is shifted to 15-20 m. The cause of the formation of this warm layer is not horizontal heat convection but a vertical downward shift of a groundwater body. This is because the temperature distribution in the 10-15 m depth layer in December does not show a horizontal temperature gradient effective enough to explain a warm heat convection which will raise the temperature in March. Since the depths of wells for snow-melting are deeper than 20 m and the water table drops are 5-10 m in winter, the warm shallower groundwater body shifts downward in response to pumping in deeper layers. The warm layer appears at the 15-20 m depth in W1 because of a larger drop in the water table.

4-3 Responses of subsurface temperature to hydrological events

In this section, the responses of groundwater temperature to hydrological events which relate to seasonal changes in subsurface temperature (Sections 4-1 and 4-2) are shown. Changes in soil temperature caused by infiltration of snowmelt water and in groundwater temperature caused by infiltration of rainfall are shown in Sections 4-3-1 and 4-3-2, respectively. In addition, the responses of groundwater temperature to pumping are indicated in Section 4-3-3.

4-3-1 Changes in soil temperature caused by infiltration of snowmelt water

Figure 19 indicates the changes in the depth of snow cover, together with the daily mean of air temperatures and soil temperatures at 4, 20, 40, 80, 120 and 170 cm depths at point W15. During the snowy season, the soil temperature at the depth of 4 cm, which is very close to the surface, was maintained at 0 °C owing to the effects of the snow cover and the temperature gradient showed a decreasing trend. There were some days with falling soil temperature from the surface to a depth of 170 cm. Judging from the agreement between the time when soil temperature falls and the time when the snow depth decreases and air temperature rises, it can be seen that soil temperature falls according to the infiltration of meltwater into the soil as a consequence of rising air temperature.

Diurnal changes in air and soil temperatures from March 9 to 20, 1983 are shown in Figure 20. It is clear from this figure that there is a close relationship between air and soil temperatures, i.e., that soil temperatures fall when air temperature rises in the day time, and recover when the air temperature falls at night, though they cannot reach the initial value.

4-3-2 Changes in groundwater temperature caused by infiltration of rainfall

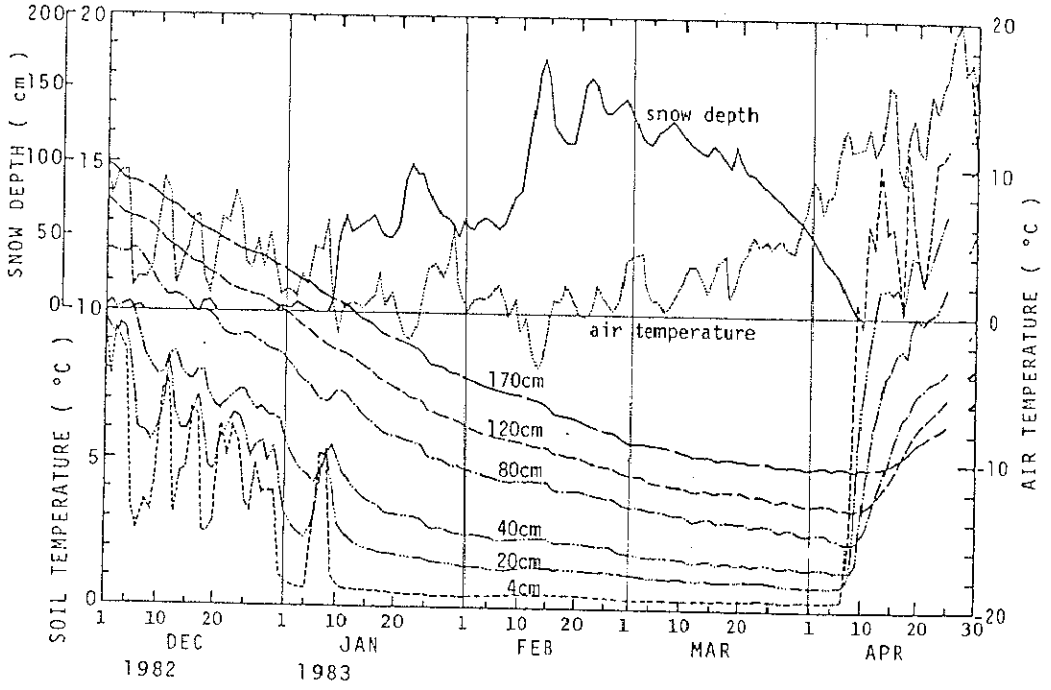

Figure 19 Changes in air temperature, snow depth and soil temperature at each depth.

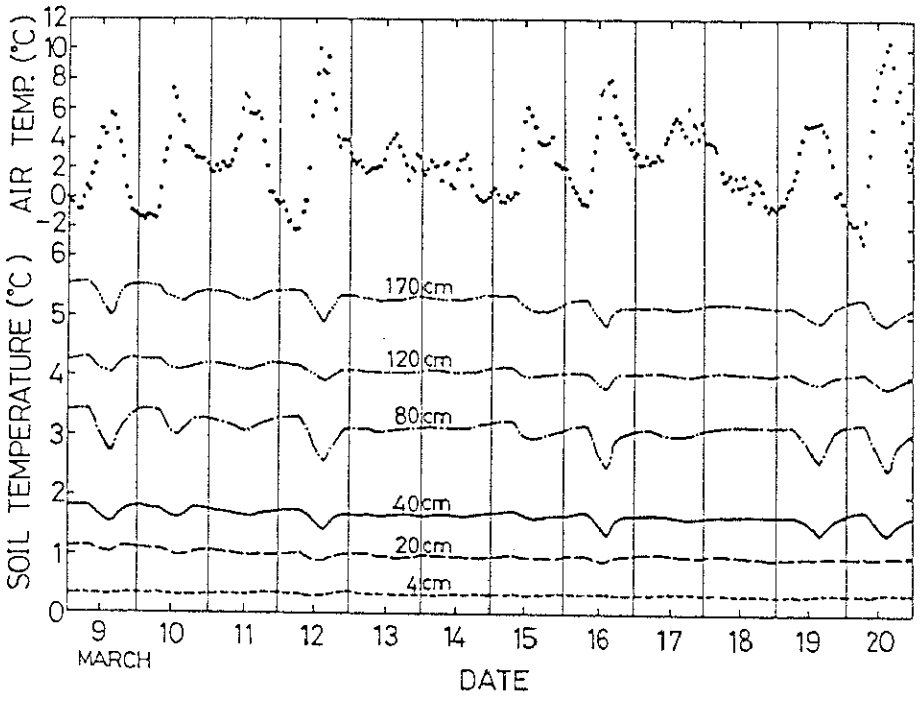

Figure 20 Diurnal changes in air and soil temperatures at each depth from March 9 to 20, 1983.

Figure 21 shows the responses of groundwater temperature at the four typical wells to rainfall with 156 mm from August 27 to September 5, 1985. This figure is shown as the isoplethes based on values observed at one-week intervals. The dotted lines in Figure 21 show the linked ones with the peak of rainfall, the time of rising groundwater level and the time of falling isothermal lines. That is to say, these dotted lines indicate the mean infiltration rate of rainfall into the ground. However, these lines do not indicate that rainfall reached these depths, but mean that subsurface water moved at each depth at each time. The infiltration rate for 156mm rainfall at well W15 of the A type is 0.88 m/day. The infiltration rates for the same rainfall at wells W18 of the B type and W31 of C type are 0.42 and 0.50 m/day, respectively.

Distribution of the infiltration rate to 156mm rainfall is shown in Figure 22. The value is large in the southern area, and small in the region near the river, in the urban area and in the northern area.

4-3-3 Responses of groundwater temperature to pumping

Figure 23 indicates the response of groundwater temperature at well W11 caused by the pumping of groundwater for melting snow. From this figure, it can be seen that the isothermal lines fall corresponding to the falls of groundwater level caused by pumping of the groundwater and that they recover during rising of the groundwater level.

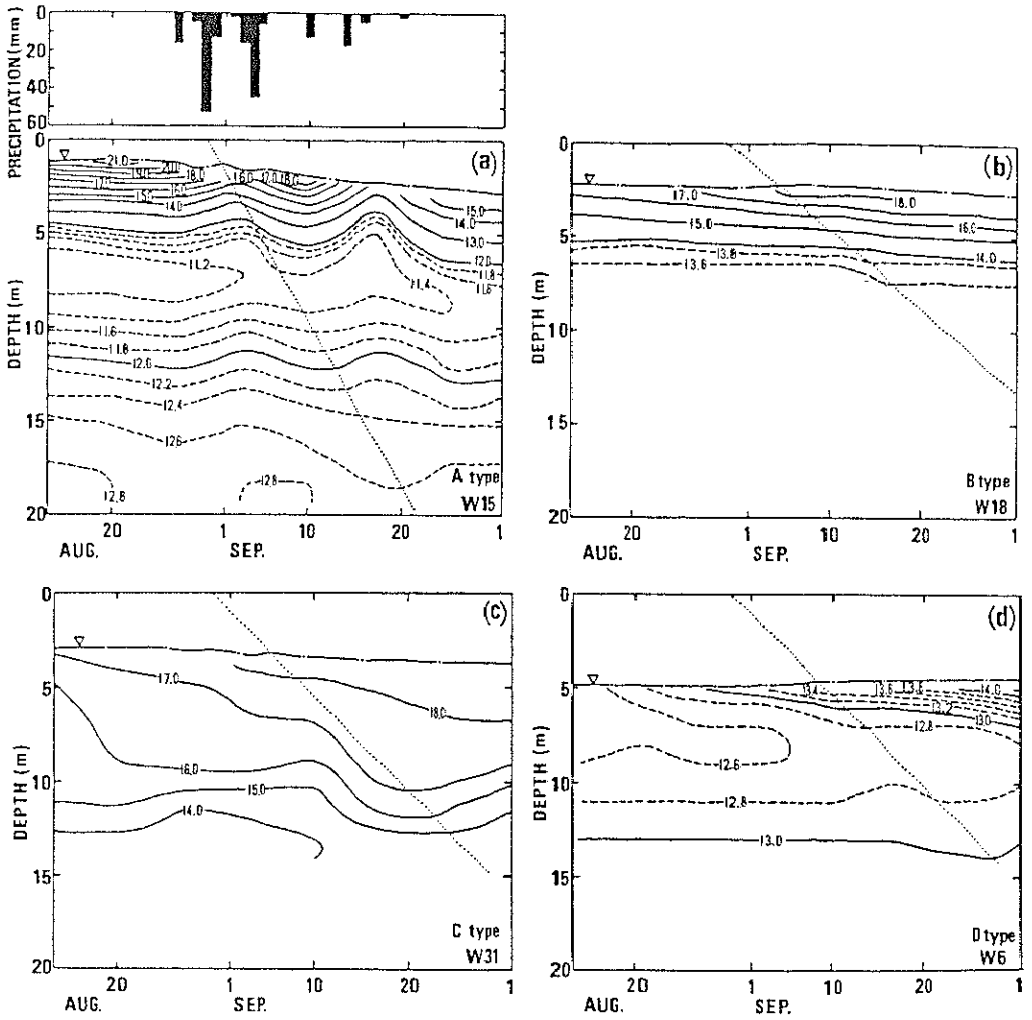

Figure 21 Responses of groundwater temperature (°C) to rainfall.

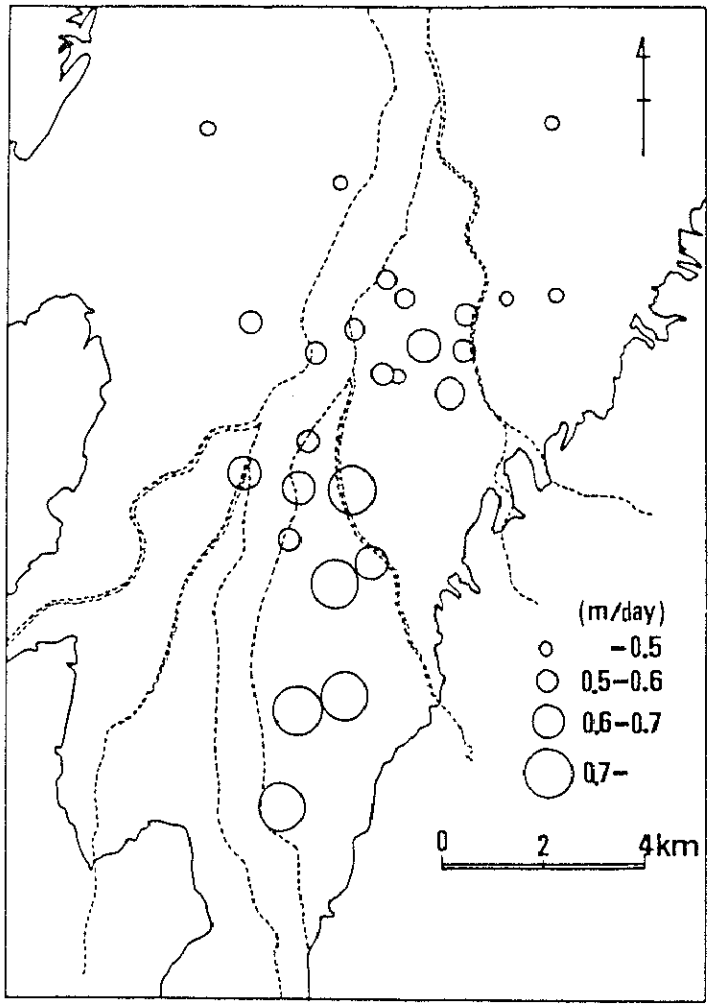

Figure 22 Distribution of the infiltration rate for 156mm rainfall.

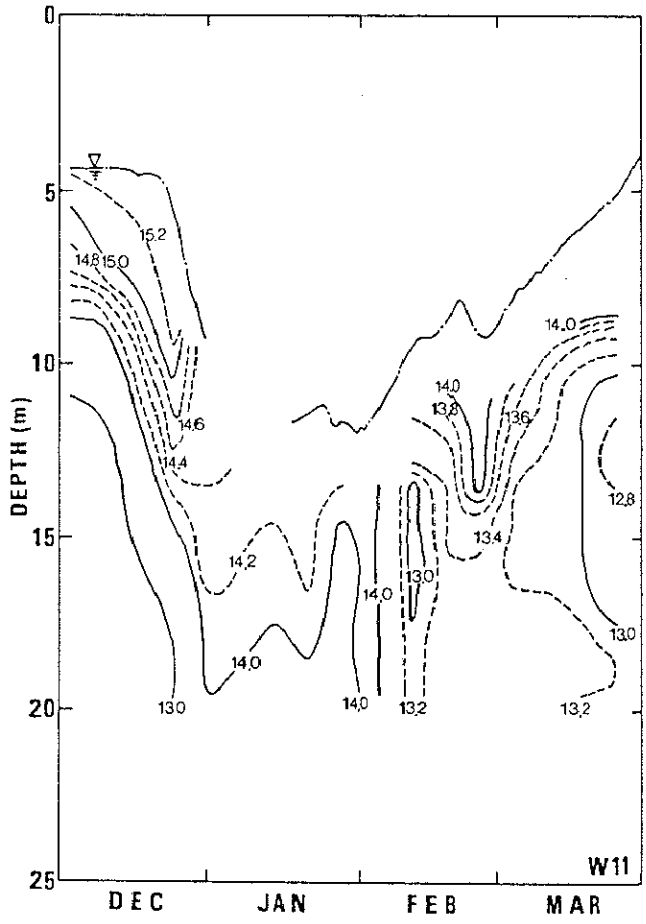

Figure 23 Responses of groundwater temperature (°C) caused by pumping at well W11.

That means, thermally stratified groundwater body shifts vertically, induced by pumping from deeper layers.

Figure 24 shows the distribution of the falling depth of the isothermal lines caused by the pumping of groundwater during the snowy season in 1984-1985. These depths were obtained from the difference between the depth of the isothermal line on the first of December and that of January. It can be seen from Figure 24 that the falling depths of the isothermal lines correspond to the falling depths of the groundwater level as can be seen in Figure 13. The wells in which the falling depth of the isothermal lines is large, are located in the urban area where the D type wells are located.

4-4 Secular variation of subsurface temperature

Specific hydrological and climatological conditions compared with those in normal years and the secular variation of groundwater temperatures at each depth in the four types of wells classified in Section 4-2-3 are shown in this section.

4-4-1 Changes in air temperature, precipitation, snowfall and groundwater level

Figures 25 and 26 show the secular variation of the deviation of precipitation and air temperature from 1982 to 1985, the depth of snowfall, water temperature of the Shinano River and the groundwater level at typical wells of the four

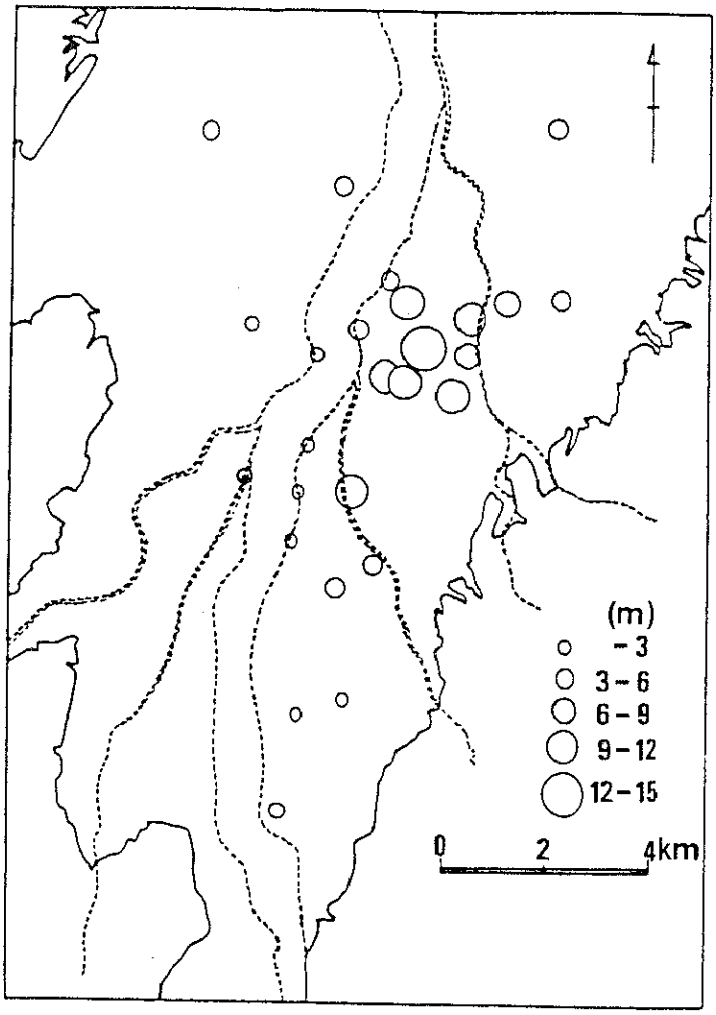

Figure 24 Distribution of the falling depth of isothermal line caused by pumping.

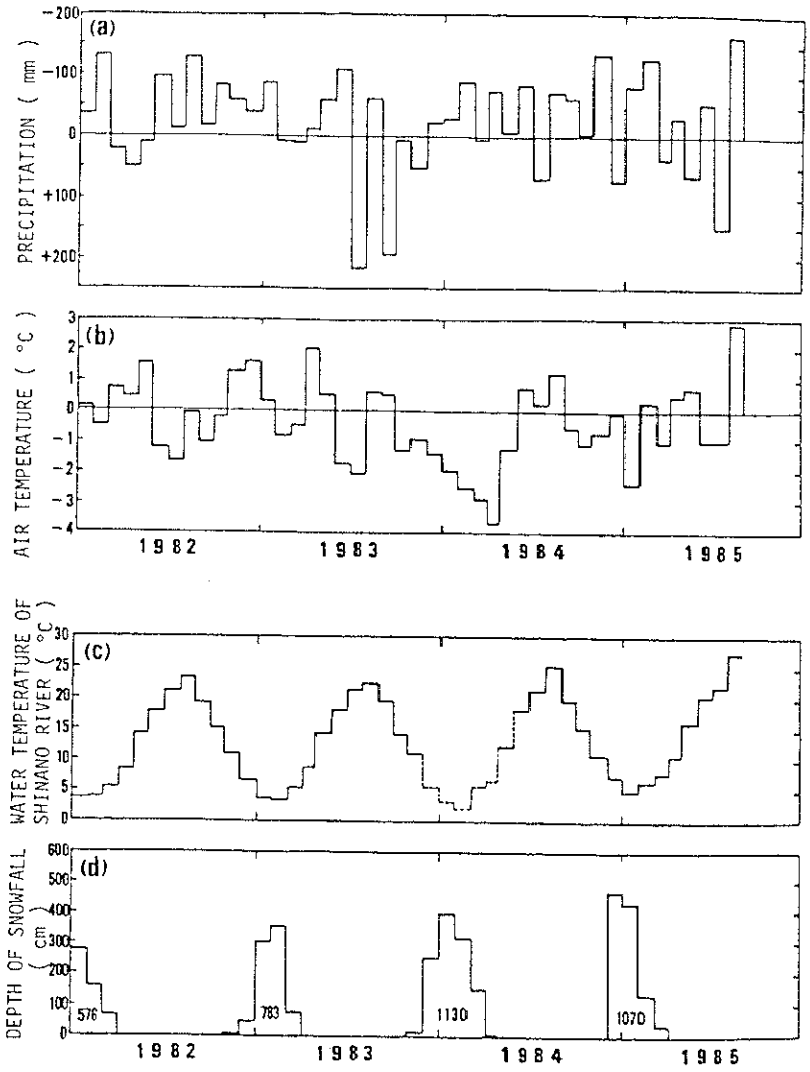

Figure 25 Secular variations of the deviation of precipitation and air temperature, water temperature of the Shinano River and the depth of snowfall.

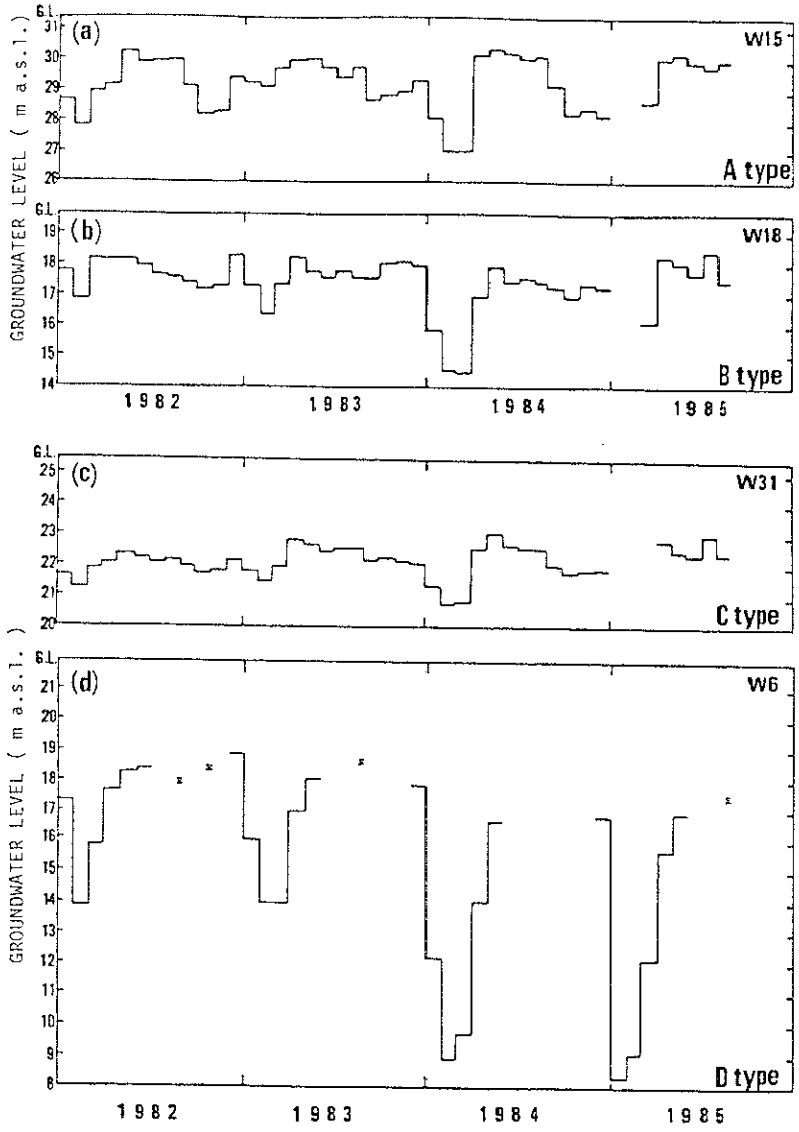

Figure 26 Secular variations of groundwater level at four typical wells.

types classified in section 4-2-3. The broken line in Figure 25-c shows the estimated water temperature from the relationship between air temperature and water temperature of the Shinano River. Blanks in Figure 26 show the periods when there was insufficient measurement, and the marks in Figure 26-d show the groundwater level when the groundwater temperature was measured. The specific hydrological and climatological conditions compared with those in normal years are as follows: plenty of rainfall in the summer of 1983 (Figure 25-a), low air temperature in the winter of 1984 (Figure 25-b) and heavy snowfall in 1984 and 1985 (Figure 25-d). In the summer of 1983, the monthly precipitations of July and September were larger by 200 mm than the value of a normal year. During the winter from 1983 to 1984, the monthly mean of the air temperature was from 1 to 4 °C lower than the value of a normal year. Depths of snowfall during winter from 1983 to 1984 and from 1984 to 1985 are larger than the values of the preceding two years. Then, the groundwater levels during those two winter seasons are lower than the levels of preceding two years, because of increased groundwater pumpage for melting the snow cover.

4-4-2 Secular variation of groundwater temperature

Figure 27 shows the secular variations of groundwater temperatures at each depth in the wells W15 of A type, W18 of B type, W31 of C type and W6 of D type. It can be seen from Figures 25 and 27 that the groundwater temperature responds

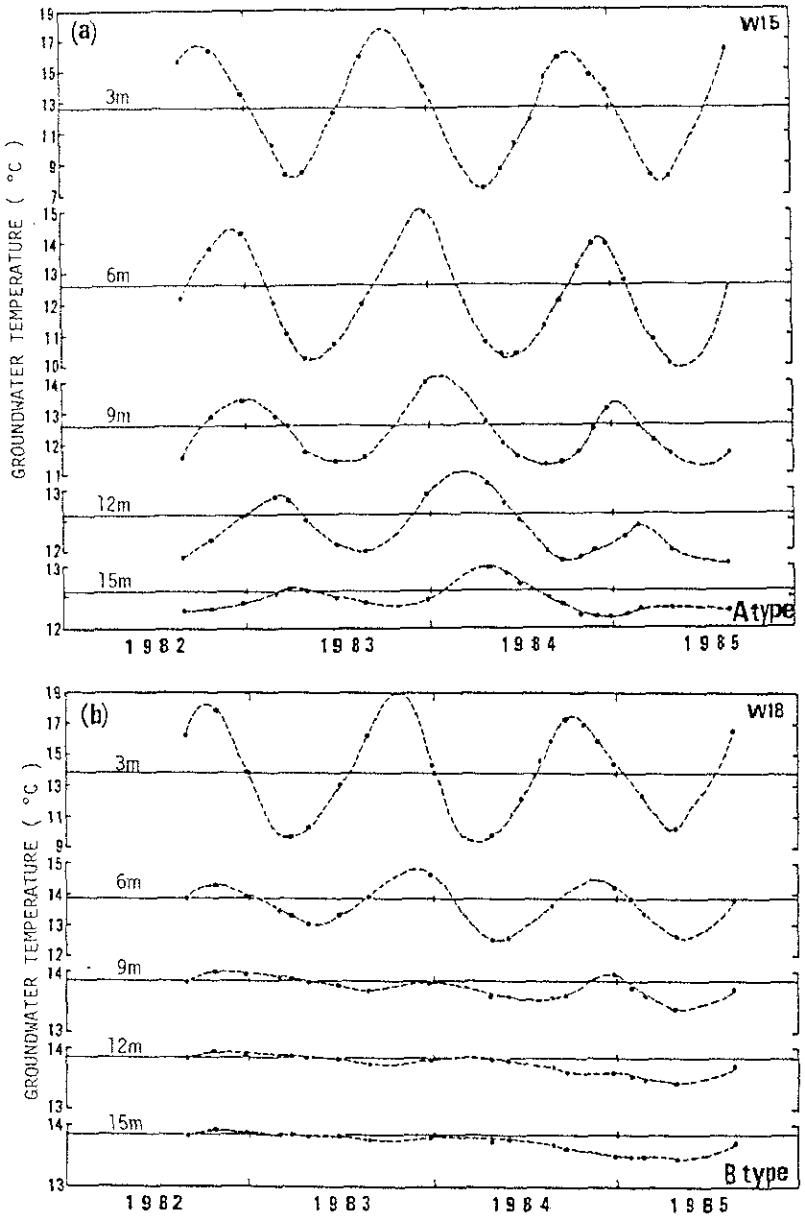

Figure 27 Secular variations of groundwater temperature at each depth.

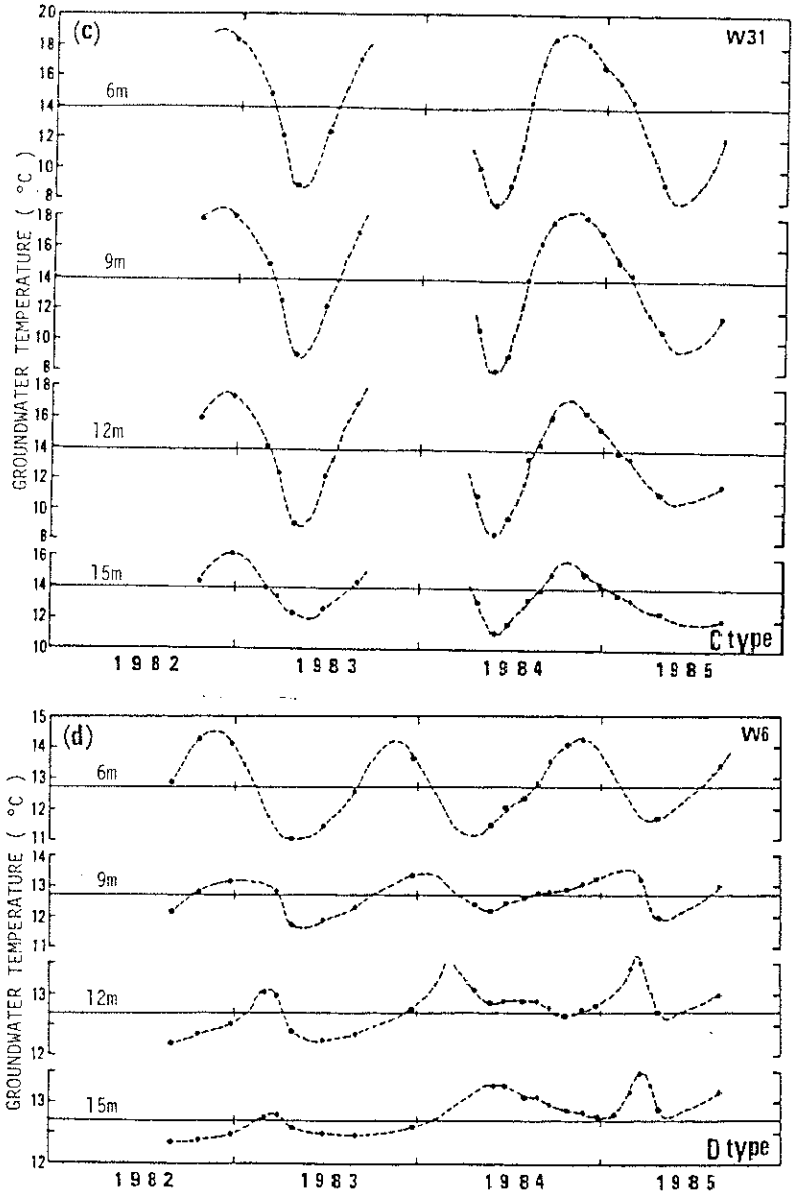

Figure 27 (continued)

sensitively to specific hydrological and climatological conditions. That is to say, the increase in groundwater temperatures is larger (Figure 27-a) than that of the normal year due to the infiltration of heavy rainfall in the summer of 1983 (Figure 25-a) at well W15, and the decrease is larger (Figure 27-b) in the winter of 1984 due to the infiltration of water under the lower temperature condition of the ground surface (Figure 25-b). The influence extends to deeper than the 10 m depth at well W15 of A Type.

It can be seen from Figure 27-c that the groundwater temperature at each depth was the lowest in May, 1984. This is caused by the seepage of cold water from the Shinano River. This is because the water temperature of the Shinano River was the lowest in February, 1984 when the groundwater level in the urban area was the lowest due to the heavy extraction of groundwater through wells.

Corresponding to the increase of the falling groundwater level in 1984 and 1985 (Figure 26-d) caused by increased pumpage for snow melting, the increase of the groundwater temperature during the winter at a depth from 9 to 15 m at well W6 is larger (Figure 26-d) than the value of the preceding year.

V. NUMERICAL ANALYSES OF SUBSURFACE TEMPERATURE DISTRIBUTION

Numerical analyses of regional differences and changes in observed subsurface temperatures are indicated in this chapter. In the unsaturated zone, changes in the soil temperature are analyzed by numerical simulation in Section 5-1. In the saturated zone, four characteristic types of temperature-depth profiles shown in Section 4-2-3, are analyzed using the one-dimensional heat conduction-convection equation in Section 5-2, and vertical two-dimensional analyses are indicated in Section 5-3.

5-1 Percolation of soil water

Changes in the soil temperature caused by the percolation of the soil water are analyzed by the numerical method in this section. First, a model of heat transport which contains not only heat conduction and convection but also the heat exchange between water and soil particles, is indicated in Section 5-1-1. Second, the numerical simulation of changes in soil temperature caused by the infiltration of snowmelt water are performed using the model and observed values of parameters for calculation in Section 5-1-2.

5-1-1 Model of soil water movement

The mechanism of the heat transport process differs when

there is mass transport. In the absence of mass transport, heat is transported only by heat conduction. In contrast, when there is mass transport, heat is transported by both heat conduction and convection. As can be seen in Figure 12, the ground surface temperature is lower than the soil temperature and the gradient of soil temperature is steep during the snow season. Thus, the influence of heat exchange between solid and fluid phases after soil water movement cannot be considered negligible. Therefore, the equation (3) of heat conduction and convection (Stallman, 1963) should be modified to take this effect into consideration.

Figure 28 shows a heat transport model in an element volume, dx;dy;dz of permeable material, which is assumed to be isotropic and homogeneous. In this study, the soil is assumed to be saturated, because the percentage of air and water vapor is small during the snowmelt season. The soil is divided into three parts, solid, mobile and immobile waters. Heat transport equations for mobile water, and for immobile water plus soil particles are expressed as follows, respectively:

$$\Theta m \cdot cw \cdot \rho w \frac{\partial Tw}{\partial t} = \Theta m \cdot kw \frac{\partial^2 Tw}{\partial z^2} - \Theta m \cdot cw \cdot \rho w \cdot Vz \frac{\partial Tw}{\partial z} + h \cdot ai(Ts-Tw) \quad .....(8)$$

$$(1-\Theta m) \cdot cs \cdot \rho s \frac{\partial Ts}{\partial t} = (1-\Theta m) \cdot ks \frac{\partial^2 Ts}{\partial z^2} - h \cdot ai(Ts-Tw) \quad .....(9)$$

where Θm and T are the mobile water content and temperature; c, ρ, k and Vz are specific heat, density, thermal

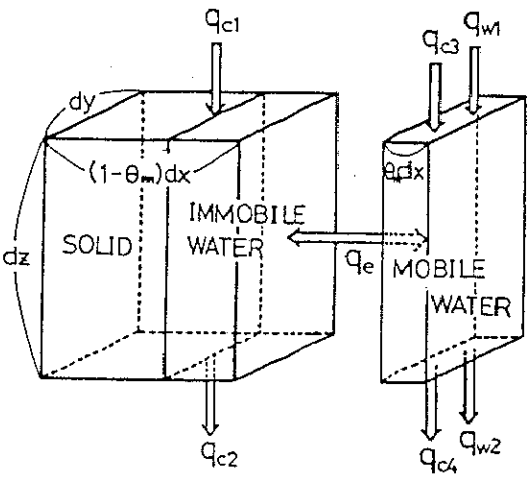

HEAT CONDUCTION: $q_{c1}-q_{c2}, q_{c3}-q_{c4}$

HEAT CONVECTION: $q_{w1}-q_{w2}$

HEAT EXCHANGE : q_e

Figure 28 Schematic diagram of heat transport in soil.

conductivity and velocity of mobile water in the z direction, respectively. Further, h and ai are the heat transfer coefficient and the interfacial area per unit volume, subscripts s and w denote solid plus immobile water and mobile water, respectively.

5-1-2 Numerical simulation of change in soil temperature

When the sensor of a thermometer is inserted into a soil section, it cannot pass into the soil particle and it is difficult for immobile water to be in contact with the surface of the sensor because of the adsorptive force of soil particles. Therefore, it is considered that the temperature measured by the thermometer is nearly equal to Tw in equations (8) and (9).

Generally, soil water is divided into bound and free waters, and it is considered that the boundary is between pF 3.0 and 4.2 (Hillel, 1971). Since the estimated line breaks at about 31 % of the water content and the pF value at the break point is about 3.5 (Taniguchi and Kayane, 1986), it is assumed that 31 % of the soil water content may be considered to be the immobile water content. The thermal conductivity ks of solid plus immobile water of 31 % was estimated from the regression line to be about 2×10^{-3} cal/cm.s.°C. The heat capacity of solid plus immobile water is estimated by the following equation:

$$Cs\,\rho s = 0.54\,f_1 + 1.0\,f_2 \qquad \text{.....(10)}$$

where the solid ratio f_1 was 0.48 and the ratio of immobile water content f_2 was 0.31.

Since it is difficult to solve equations (8) and (9) analytically, soil temperatures are simulated using a computer. The numerical simulation is based on a backward finite difference approximation, and the Gauss elimination is used for the calculation.

The soil and groundwater temperatures at the time when the temperature began to fall simultaneously from the surface to a depth of 170 cm (Figure 19), are used as the initial conditions for calculation. It is assumed that Ts is equal to Tw at t = 0. The soil temperature at the surface and the groundwater temperature at the depth where the temperature gradient is nearly zero are used as the upper and lower conditions, respectively. The term h·ai is considered to be negligible in the calculation for the period during which soil temperatures fall, because soil water moves quickly. Although the percolation velocity Vz changes according to the rate of the infiltrated meltwater, it is assumed that Vz remains constant while the soil temperature is falling. The assumption is based on a linear decrease in the soil temperature at any depth with nearly the same gradient (Figure 20).

Diurnal changes in the soil temperature are simulated under the conditions and procedures mentioned above, for March 1, 9, 15, 23, 30 and April 6, because the vertical distributions of the groundwater temperature were measured on

these dates. Figure 29 shows comparisons of calculated and measured soil temperatures at the depths of 40, 80 and 120 cm from the beginning of the soil temperature decrease up to 15 hours later on March 9 and 15. The best fitted values (within 0.1 °C) on March 9 and 15 are obtained when the percolation velocities of mobile water are 1.7 and 1.5 cm/hour, respectively, from the beginning of the soil temperature decrease up to 6 and 5 hours later, and when the values of h·ai are 0.02 and 0.04 cal/cm·h·°C, respectively.

The changes in the soil temperature on the six days when the calculations were performed, can be simulated within 0.2 °C using values of h·ai which are between 0.02 and 0.04 cal/cm·h·°C. Simulated infiltration rates and snowmelt rates on the six days are shown in Table 2. The infiltration rate I is the product of the mobile water content, the percolation velocity and the consecutive hours of infiltration in one day. The snowmelt rate S is the product of the water equivalent of snow cover in an element volume and difference of the snow depth. The ratios of I to S were between 0.42 and 0.83.

The ratios of volume of the infiltrated water to rainfall using the same model were between 0.28 and 0.67. The means of the ratio of the infiltrated water to the snowmelt water and rainfall are 0.65 and 0.43, respectively. Therefore, the ratio of the infiltrated water to the snowmelt water is about 1.5 times as large as that to the rainfall.

5-2 One-dimensional groundwater flow

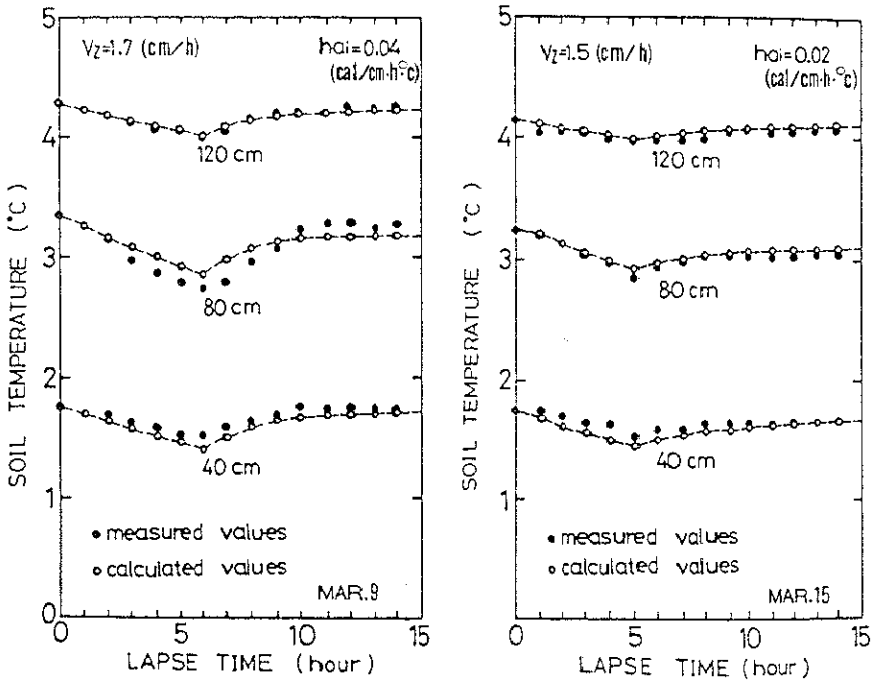

Figure 29 Comparisons of measured and calculated soil temperatures on March 9 and 15, 1983.

Table 2 Calculated values of infiltration and snowmelt rates

	Mobile water content (%)	Percolation velocity ($cm\ h^{-1}$)	Consecutive hours (h)	Infiltration rate (I) ($cm\ day^{-1}$)	Snowmelt rate (S) ($cm\ day^{-1}$)	I/S
Mar. 1	12	1.5	7	1.26	2.39	0.53
Mar. 9	14	1.7	6	1.43	1.90	0.75
Mar.15	14	1.5	5	1.05	1.94	0.54
Mar.23	17	0.8	6	0.82	1.93	0.42
Mar.30	19	1.6	7	2.13	2.56	0.83
Apr. 6	19	2.8	8	4.26	5.10	0.84

Regarding the temperature-depth profiles in the saturated zone, it became clear in Section 4-2-3 that the profiles are classified into four types. After showing the adequacy of one-dimensional analyses, the temperature-depth profiles of A and B types are analyzed in Section 5-2-1 using the vertical one-dimensional conduction-convection equation. The profiles of the C and D types are analyzed using the horizontal and vertical conduction-convection equations in Sections 5-2-2 and 5-2-3, respectively.

5-2-1 Vertical groundwater flow in the recharge and discharge areas

The response of the groundwater temperature to rainfall was shown in Section 4-3. In order to clarify the effect of rainfall on the depth to the isothermal layer, Figure 30 shows the relationships between precipitation and the depth to the boundary of layer in which the groundwater temperature changes more than 0.1 °C because of the infiltration of rainfall at W15, W18 and W31. Broken lines in this figure show the depths of the isothermal layer at each point. The ratio of the depth approximated by quadratic equation to the depth of isothermal layer is 0.92 at well W15 (Figure 30-a). In addition to this, Taniguchi (1985) clarified that horizontal groundwater flow hardly affects the groundwater temperature at well W15. Therefore, it is possible to analyze the groundwater temperature in well W15 using the

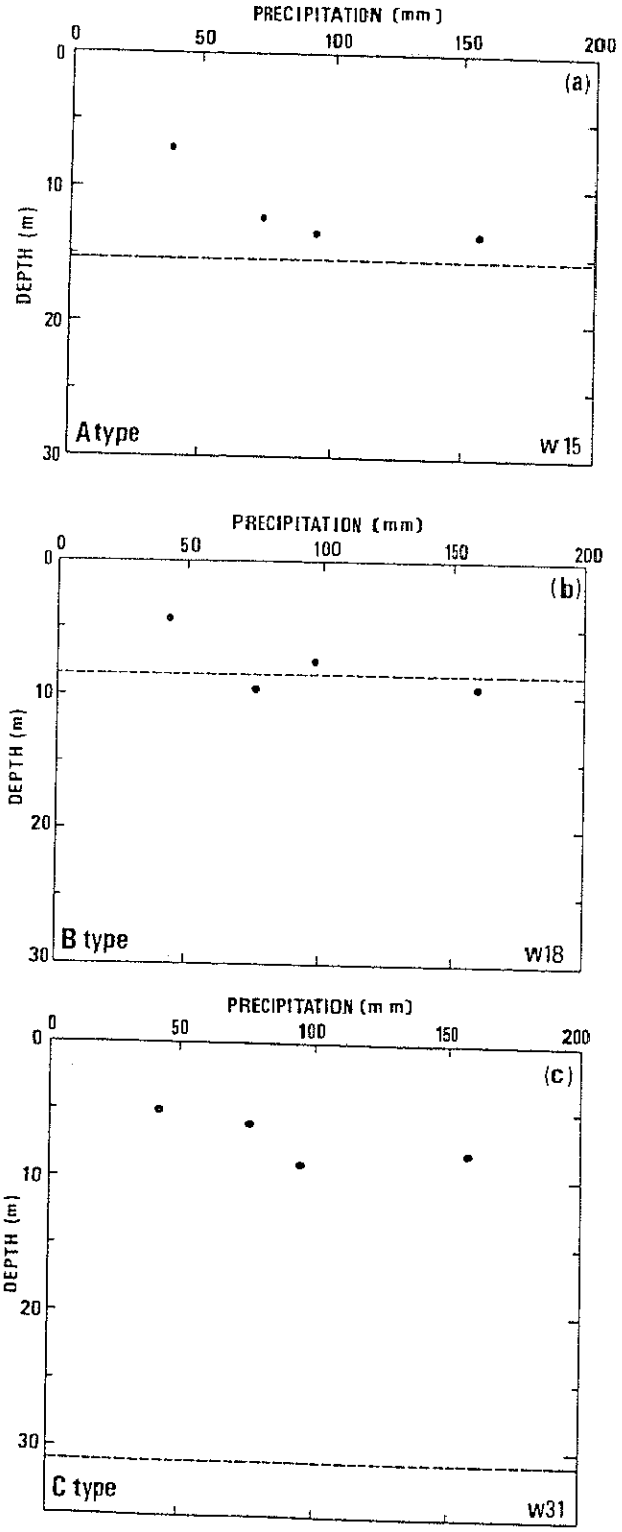

Figure 30 Relationships between precipitation and the depth to the boundary of layer in which the groundwater temperature changes more than 0.1 °C on account of infiltration of rainfall.
Broken lines show the depth to the isothermal layer.

following vertical one-dimensional equation which is converted from equation (3).

$$c_0 \frac{\partial T}{\partial t} = k_z \frac{\partial^2 T}{\partial z^2} - c_0 \rho_0 q_z \frac{\partial T}{\partial z} \qquad \text{.....(11)}$$

Figure 31 shows the seasonal changes of groundwater levels at observation well W13 which is located near well W15, at observation well W18 and the shallow wells near each observation well. From these water levels in shallow and deep wells, it is possible to calculate the vertical groundwater flux. This is because the positions of the screens in the observation wells (Table 1) are deeper than the depths of the shallow ones which are 5.6 m and 6.0 m depths at W339 and W135, respectively. At well W13 (Figure 31-a), the hydraulic head of the observation well is lower than the shallow one indicating the downward groundwater flux. In contrast, at well W18 (Figure 31-b), the hydraulic head of the observation well is higher than the shallow one, indicating the upward groundwater flux.

Vertical one-dimensional calculations are performed by using equation (11). With regard to the thermal diffusivity, the values of 4.9×10^{-3} cm^2/s in the gravel and clay layer (Boyle and Saleem, 1979), 5×10^{-3} cm^2/s in alluvial deposits (Cartwright, 1968) and 7×10^{-3} cm^2/s in medium coarse sand with gravel (Andrews and Anderson, 1979) were used in previous studies of groundwater temperature. In this study, 6×10^{-2} m^2/day is used as the thermal diffusivity because the geology of the study area consists of sand and gravel. Soil

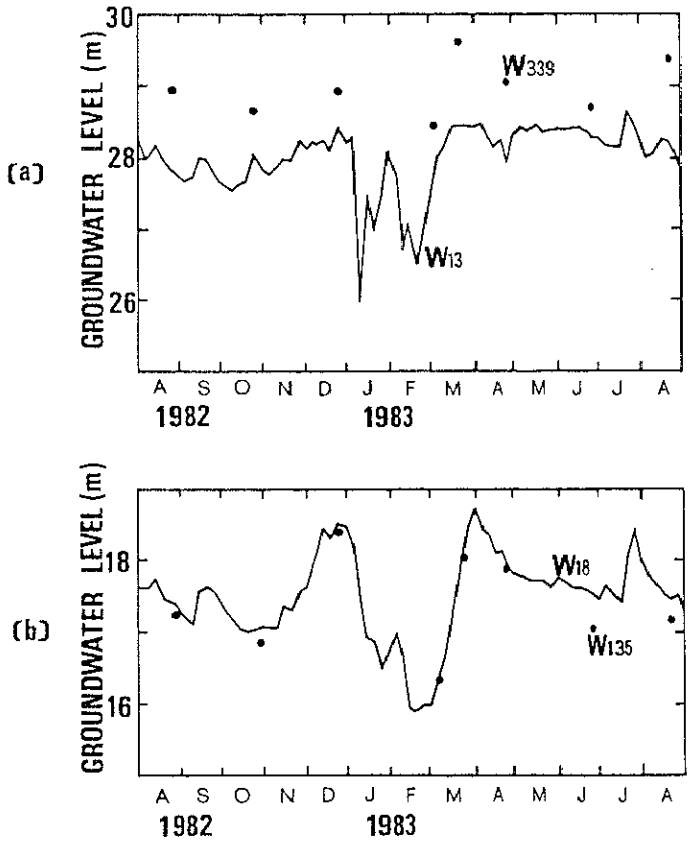

Figure 31 Seasonal changes in groundwater level at (a) well W13 and (b) well W18, and at the shallow wells near the each observation well.

temperatures at the depth of 4 cm below the surface and groundwater temperatures at the depth of 20 m, are used as the upper and lower boundary conditions, respectively. Calculations are based on a backward finite difference approximation, and repeated until the difference between the calculated temperature and that of preceding step is within 0.001 °C. Temperature-depth profiles for the A type in Figure 32-a are calculated by giving the downward groundwater flux of 0.01 m/day. The water flux is obtained by multiplying the mean hydraulic gradient at well W13 (Figure 31-a) by the hydraulic conductivity in the vertical direction which is between 0.1 and 0.01 times as small as that of the horizontal direction.

Figure 32-b shows the calculated temperature-depth profiles for the B type by giving the upward groundwater flux of 0.01 m/day. The water flux is obtained by multiplying the mean hydraulic gradient at well W18 (Figure 31-b) by the hydraulic conductivity in the vertical direction which is between 0.1 and 0.01 times as small as that of the horizontal direction. Figure 32-a and Figure 32-b show the characteristics of the temperature-depth profiles of the A type and B type wells, especially the depth to the isothermal layer. That is to say, it is clarified by calculations that the depth to the isothermal layer deepens in the recharge area and shallows in the discharge area due to downward and upward water flow, respectively.

5-2-2 Horizontal advection of groundwater flow

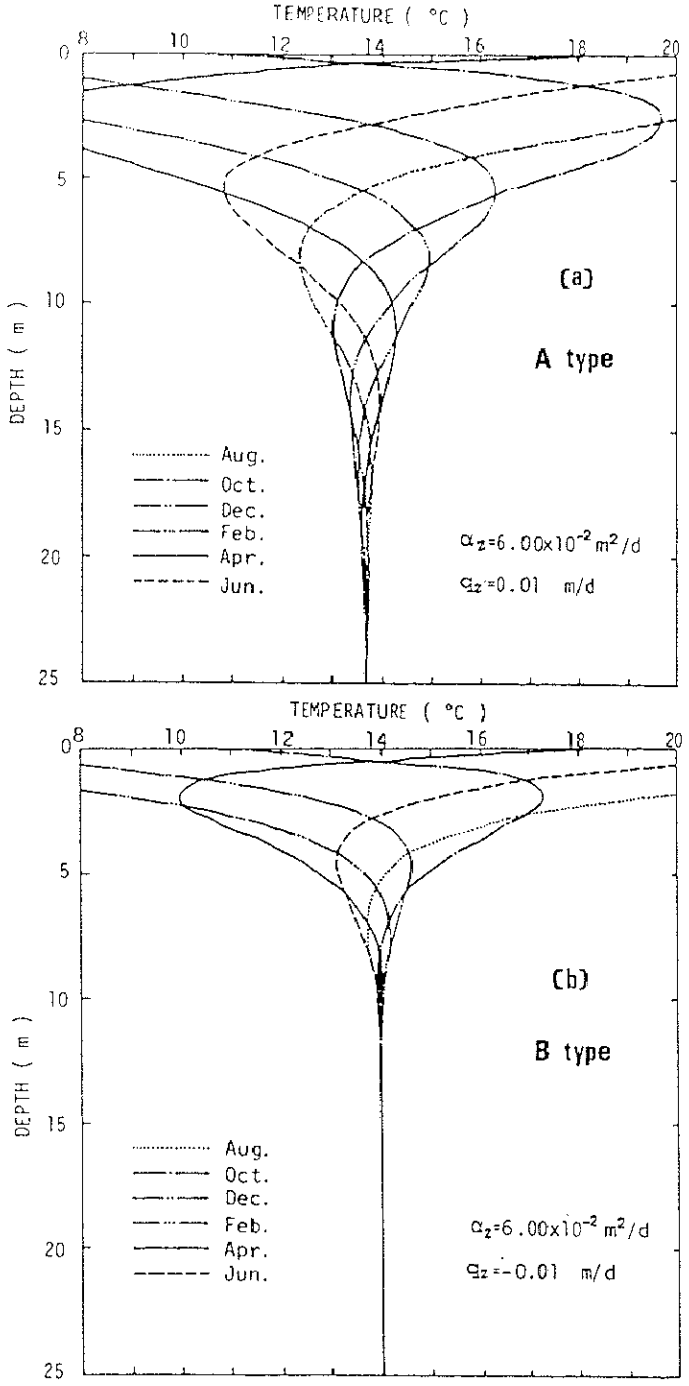

Figure 32 Calculated profiles of groundwater temperature by equation (11) for A and B type wells.

The temperature-depth profiles of well W31, which is a typical well of the C type, are not explained by vertical one-dimensional analysis as can be seen in Figure 30-c. Therefore, the numerical analyses of the change in groundwater temperatures caused by horizontal groundwater flow are made for the C type well in this section. The results of the calculations are shown in Figure 33 using the following horizontal one-dimensional heat conduction-convection equation which is converted from equation (3).

$$c\rho \frac{\partial T}{\partial t} = kx \frac{\partial^2 T}{\partial x^2} - c_0 \rho_0 qx \frac{\partial T}{\partial x} \qquad \text{.....(12)}$$

The water temperature of the Shinano River (Figure 33-a) was used as a boundary condition because the groundwater near the well W31 almost comes from the Shinano River throughout the year, judging from the configuration of the water table as shown in Figure 13. The mean groundwater temperature in the well W11 was used as the other boundary condition. Calculations are performed with different water fluxes (Figure 33-b) and thermal diffusivities (Figure 33-c) as parameters. When the water flux qx is 0.34 m/day, the observed groundwater temperatures agree with the calculated values. This flux is nearly equal to the value calculated by hydraulic conductivity and the mean hydraulic gradient of 0.003 in the region near well W31 (Figure 13). When the thermal diffusivity of the horizontal direction is 1.8×10^{-1} m^2/day, the calculated temperatures approximately coincide

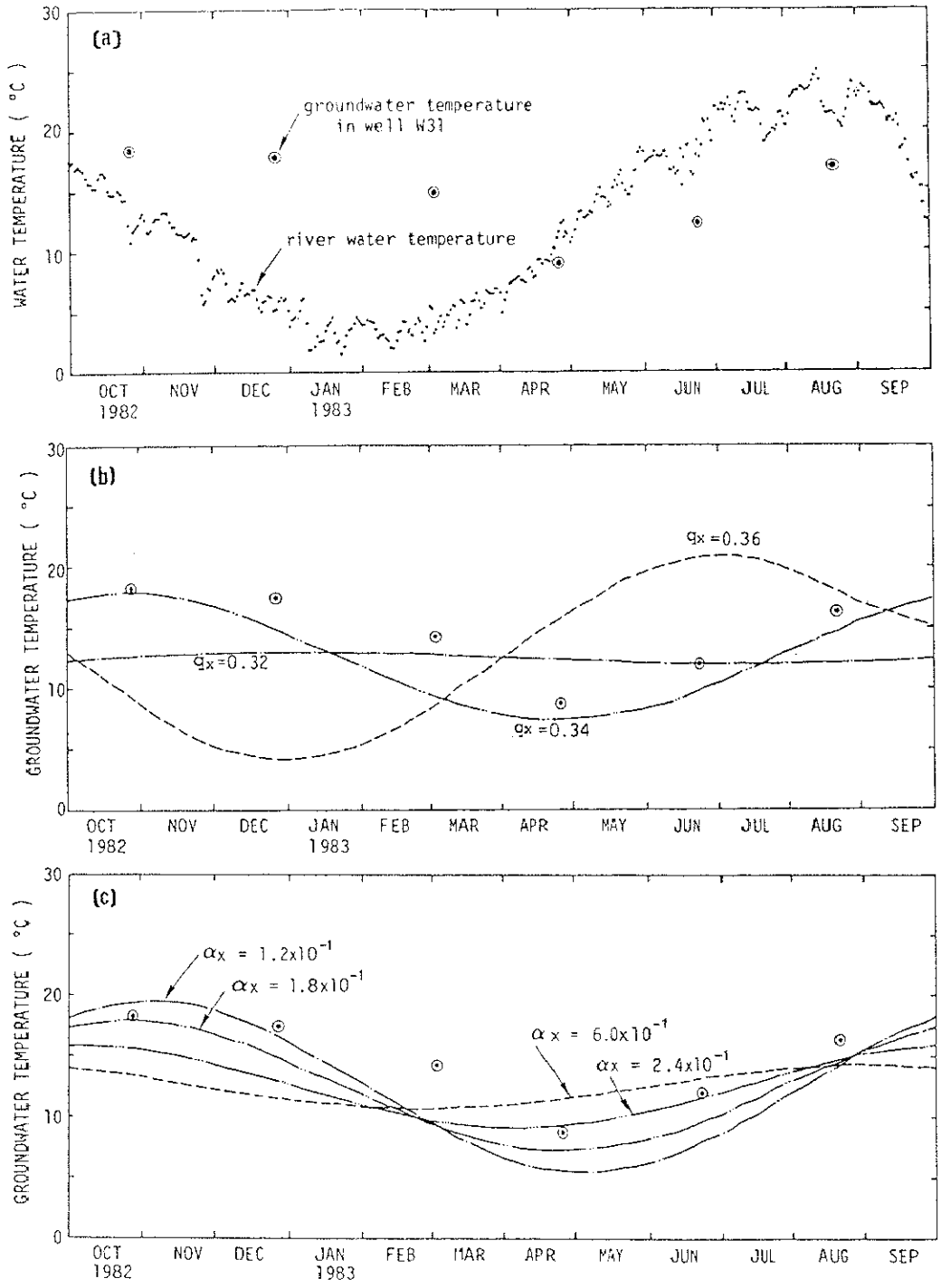

Figure 33 Seasonal changes in calculated groundwater temperature for C type well by using equation (12) and different values of horizontal flux (m/day) and horizontal thermal diffusivity (m^2/day).

with the observed ones, though the agreement in March was not good. The horizontal thermal diffusivity obtained as mentioned above is three times as large as the vertical one which is assumed to be 6.0×10^{-2} m^2/day based on previous studies.

5-2-3 Shift of groundwater body due to pumping

Figure 34 shows the results of calculations for the D type well using the vertical one-dimensional conduction-convection equation (11). In this calculation, the downward water flux of 0.08 m/day which is obtained from the effective porosity of 0.3 and the falling depth of the groundwater level, is given during January and February below the depth of 5 m. This is because the groundwater level began to fall at that depth. The temperature and the depth of warm layer in the temperature-depth profile in March indicate the characteristics of the D Type well in the urban area.

Groundwater temperatures for D type wells in each year are calculated by the same method mentioned above. Figure 35 shows the observed relationships between the differences of groundwater temperature at the depth of 12 m and the differences of groundwater level between December and February in D type wells. This figure also shows the calculated relationships between the differences of groundwater temperature at 12 m depth and the downward water flux which is given during January and February below the depths of 3, 4 and 5 m for the calculations as mentioned

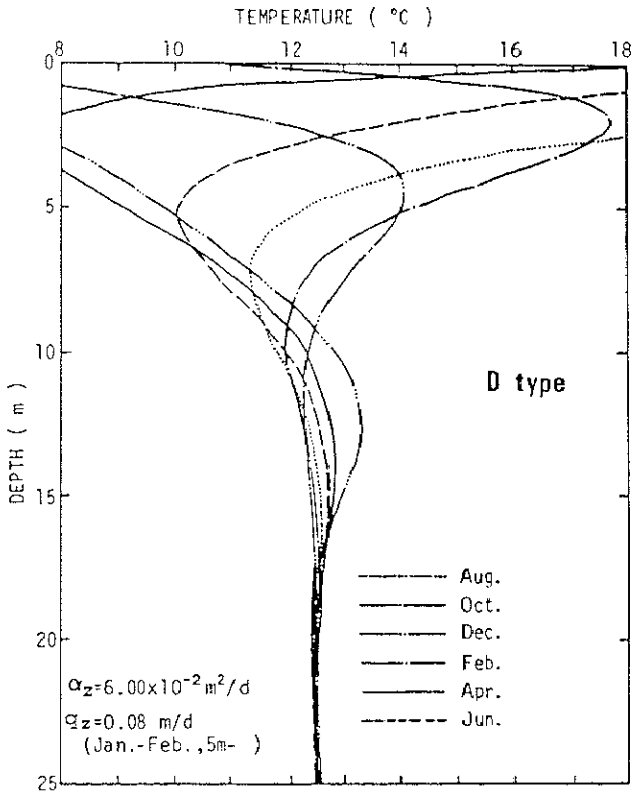

Figure 34 Calculated profiles of groundwater temperature by equation (11) for D type well.

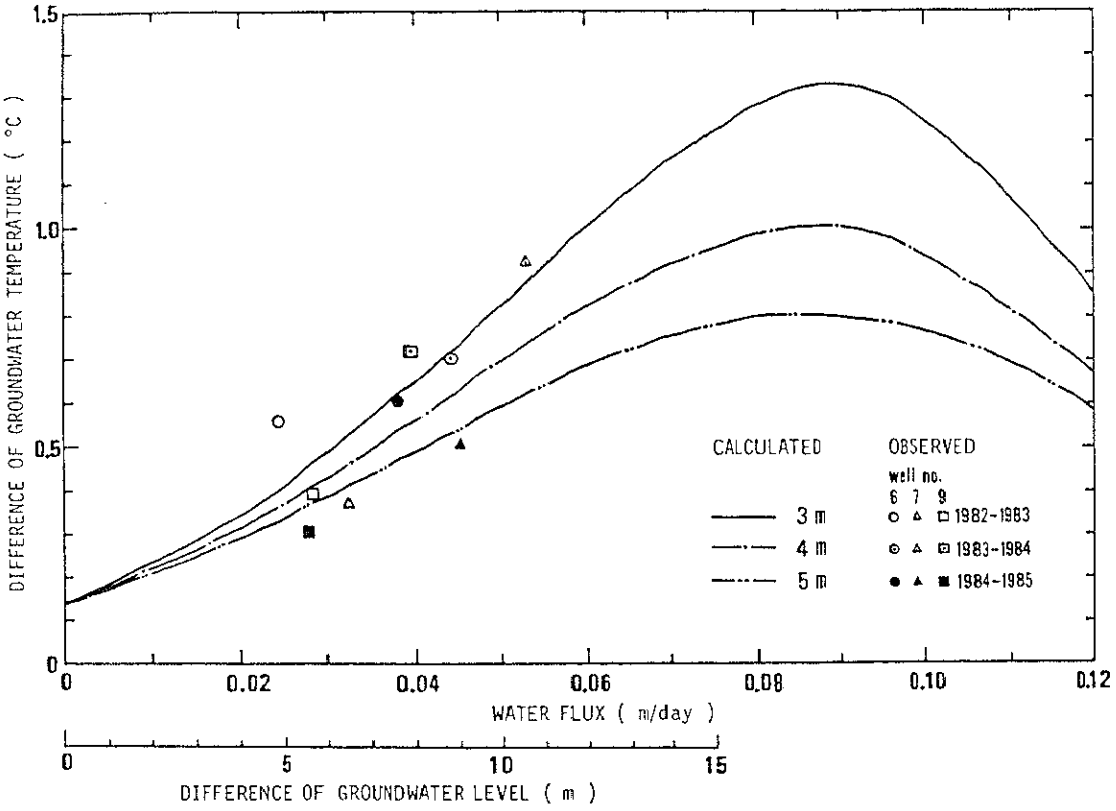

Figure 35 Observed relationships between the differences of groundwater temperature at the depth of 12 m and the differences of groundwater level between December and February in D type wells, and calculated relationships between the differences of groundwater temperature obtained by using equation (11) and downward water flux which is given for calculation during January and February below the depths of 3, 4 and 5 m.

above. That means, the numbers of calculated lines in this figure indicate the depth where the groundwater level began to fall. When the effective porosity is assumed to be 0.3, the falling groundwater level of 10 m during two months corresponds to the downward water flux of 0.05 m/day. In this figure, the observed values at each point in each year correspond to the calculated values. Therefore, it can be seen that the warm layer caused by pumping depends on the groundwater level before pumping and the falling depth of the groundwater level.

5-3 Vertical two-dimensional groundwater flow

In Figure 15 of Section 4-2-2, seasonal changes in the groundwater temperature in the vertical cross sections were shown. In order to clarify the effect of two-dimensional groundwater flow on groundwater temperature, the results of analysis in the vertical north-south section are shown in this section. Figure 36 indicates the grid spacing for the calculation along A-B in Figure 6 and the seasonal variation of the change in the heat storage caused by heat convection. The difference between the calculated groundwater temperature obtained by using a two-dimensional heat conduction equation which is converted from equation (1) and the observed one, is shown in this figure as the change in heat storage by the heat convection. Soil temperatures at the depth of 4 cm below the surface and the groundwater temperature gradient of 0.025 °C/m, are used as upper and lower boundary conditions

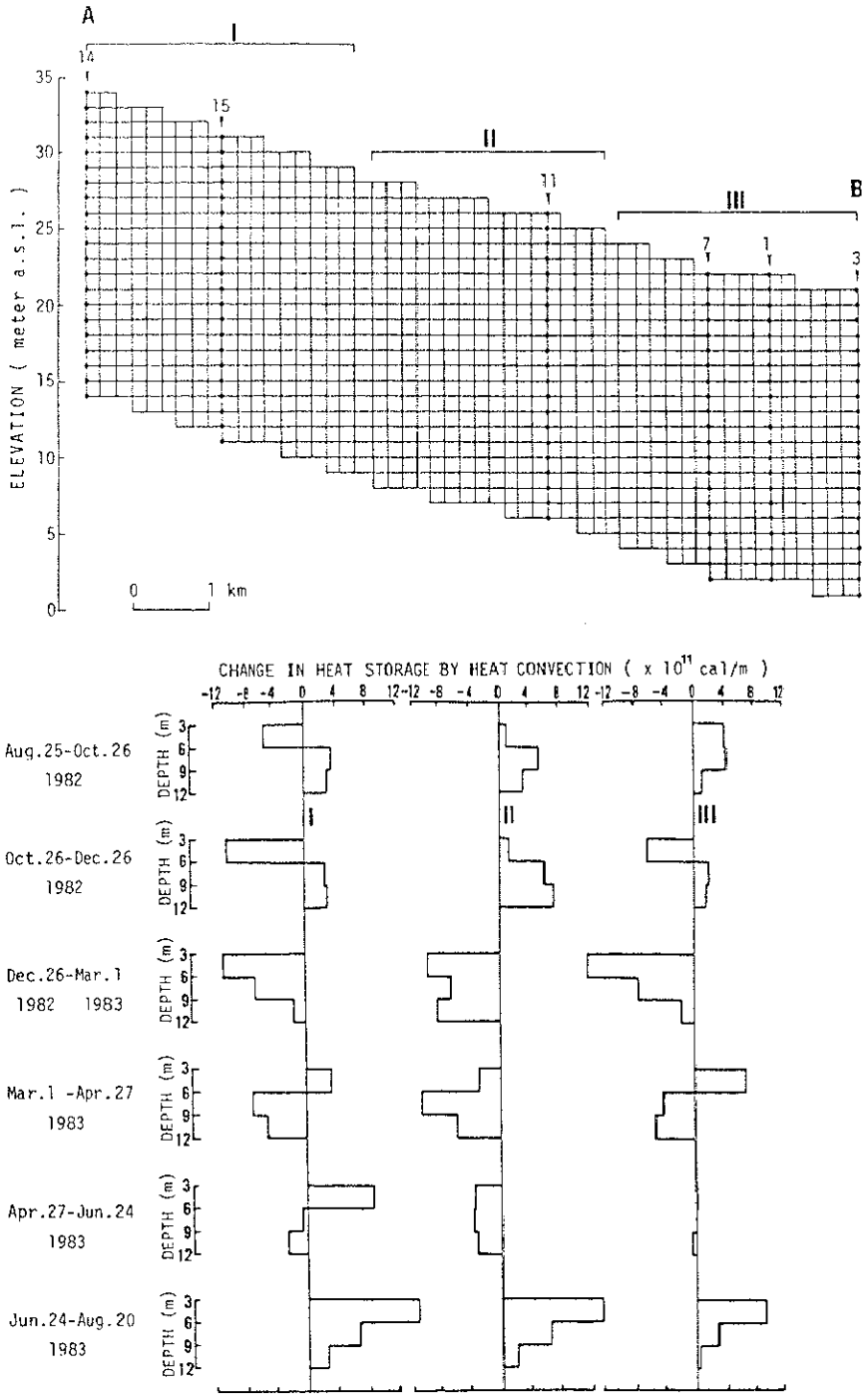

Figure 36 Grid spacing for calculation along A-B in Figure 6 and seasonal variation of change in heat storage caused by heat convection.

for calculation.

In zone I, which is located in the southern area, the change in heat storage caused by heat convection moves from the upper layer to the lower layer. This means that the downward heat convection mainly affects the groundwater temperature in zone I. In zone II, there is little difference of change in heat storage with depth, that is, heat storage at each depth changes in the same way. These indicate that heat convection caused by infiltration from the surface dominates in the southern area, and horizontal heat convection mainly affects the groundwater temperature in zone II. In comparing zone I with zone III, which is located in the urban area, changes in heat storage support the upward groundwater flow from the lower layer during the recovery of groundwater level after March, at the depth from 3 to 6 m. Therefore, it can be seen that the change in heat storage caused by heat convection reflects the regional groundwater flow system in which the recharge dominates in the southern area, and the groundwater flows and discharges into the northern area.

VI. DISCUSSION

Regarding the soil temperature in the unsaturated zone, it has been clarified by an experiment in the unsaturated zone using a soil column, that soil water movement in the capillary water zone takes place simultaneously at all levels whenever a wetting front reaches the upper boundary of the unsaturated capillary water zone (Sakura and Taniguchi, 1983). In the present study, judging from the soil water content and groundwater level, the unsaturated zone is almost within the capillary water zone during the snowy season because the soil consists of fine particles mostly composed of silt at the observation point (Taniguchi, 1985). Therefore, the simulation using equations (9) and (10) are performed in Section 5-1 under the condition that the infiltration velocity is constant in regard to the depth and time during the soil temperature fall.

Combarnous and Bories (1975) mentioned that the heat transfer coefficient h depends on fluid velocity and viscosity, on the thermal characteristics of both solid and fluid phases, and on the texture of the medium. When water moves quickly, it is considered that the heat transfer coefficient h is very small. Therefore, $h \cdot ai$ is considered to be negligible in the calculation for the period in which soil temperatures fall simultaneously from the surface to a depth of 170 cm (Figure 29).

In this study, $h \cdot ai$ was determined by numerical

simulation because it was difficult to measure the heat transfer coefficient (h) and interfacial area (ai) in the field. Then, infiltration rates were calculated for six days during which groundwater temperatures were observed. Therefore, if the groundwater temperature during the snow cover season is known, it will be possible to calculate the snowmelt rate during the whole winter in the snowy area, based on the soil temperature change. In the future, it will be necessary to determine the heat transfer coefficient based on the physical characteristics of the soil and on the flow condition of water using a soil column in which heat and water flows can be controlled.

Regarding the results in the saturated zone, Figure 37 shows the distribution of the depth to the isothermal layer determined by the groundwater temperature measured at two-month intervals during a year. The depth indicates the top of the layer at which the annual change of groundwater temperature is within 0.1 °C. In this figure, the broken circles show the values obtained from the groundwater temperature measured at four-month intervals during three years. It is clear from this figure that the values are large in the southern area where the A type wells are located and the region near the river where the C type wells are located. In contrast, the depth to the isothermal layer is small in the northern and urban areas, in the north of the left bank of the Shinano River where B type wells are located and in the south of the left bank of the Shinano River where a thick clayey layer accumulated.

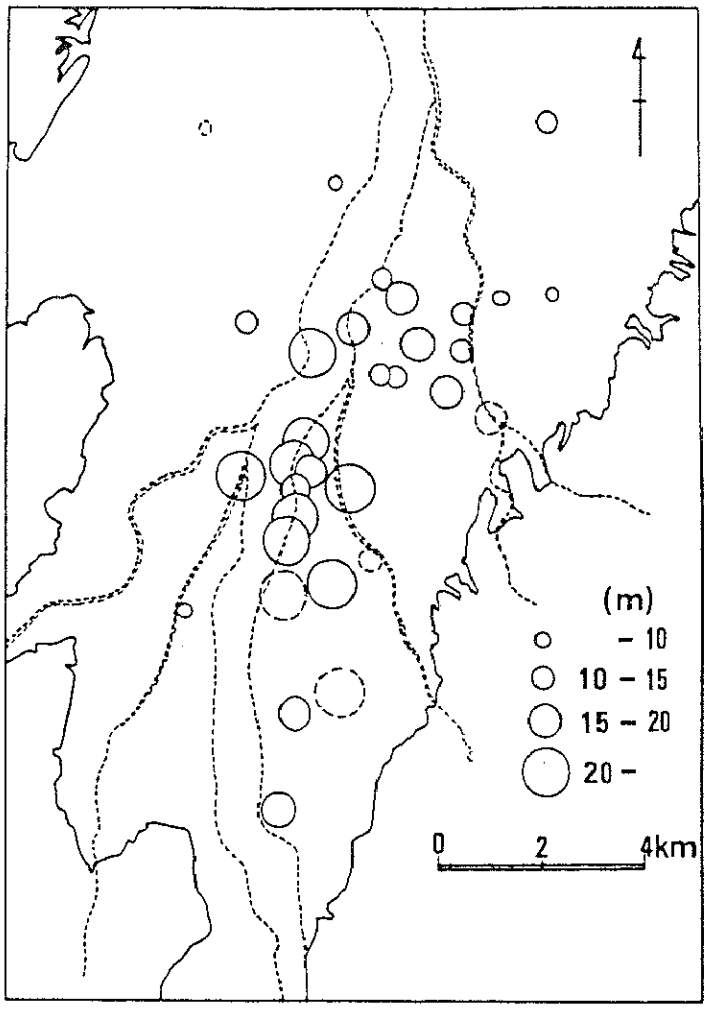

Figure 37 Distribution of the depth to the isothermal layer.

If the heat convection caused by the movement of subsurface water does not exist, the depth to the isothermal layer at every point should be the same because the subsurface temperature is formed due to the division of energy only by heat conduction. However, distribution of the depth to the isothermal layer shows the regional characteristics reflecting the three-dimensional groundwater flow.

Comparing Figure 37 with Figure 22, which indicates the distribution of the infiltration rate for 156mm rainfall, the depth to the isothermal layer corresponds to the infiltration rate except for the region near the river. That is to say, deep and shallow depths to the isothermal layer correspond to the large and small values of the infiltration rate in areas where A type and B type wells are located, respectively. However, the depth to the isothermal layer in the region near the river where C type wells are located, is deep in spite of the small value of the infiltration rate of rainfall. This means that the groundwater temperature in C type wells is mostly formed by horizontal advection as can be mentioned in Section 5-2-2.

In Section 5-2, it was clarified by the analysis considering heat convection that the difference between the temperature-depth profiles of four typical wells and the normal profiles calculated by the heat conduction theory is caused by the regional groundwater flow. Therefore, the A type is named as a recharge type which is located in the recharge area where the downward water flux dominates. This

type can be explained by the downward flow rate of 0.01 m/day throughout the year, so that, the depth to the isothermal layer is deeper by 5 m than the value obtained by the heat conduction theory. In contrast, the B type is named as a discharge type which is located in the discharge area with the upward flow rate of 0.01 m/day throughout the year, so that, the depth to the isothermal layer is shallower by 5 m than the one calculated by the heat conduction equation. In addition to these, the C type is named as an advection type in which heat convection due to the horizontal groundwater flow near the river contributes to the groundwater temperature formation. The D type is named as a pumping type which has a characteristic of warm layer at the depth of 10-15 m during the winter due to pumping for snow melting.

In Section 5-2, numerical analyses of temperature-depth profiles using one-dimensional equations (11) and (12) are performed on four types of wells. The calculated temperature agreed with the observed value regarding the depth to the isothermal layer and the warm layer in D type wells. However, the calculated subsurface temperatures did not agree well with the observed ones in the shallow layer. This is due to using a steady water flux for calculation. Though the recharge rate, discharge rate, horizontal groundwater flow rate from the Shinano River and the vertical water flow rate induced by pumping are used for calculations as constant values in this study, these flows are unsteady in fact. If the unsteady water flow can be known throughout the year, the calculated values will agree better with the observed ones.

In Section 4-4, the secular variations of groundwater temperatures for four typical wells were shown with climatological data such as air temperature, precipitation and so on. Though the change of groundwater temperature in the well of recharge type (A type) corresponds to the change of these data mentioned above, the change of temperature in the other type wells does not correspond to the change of precipitation and the air temperature. That is, when the subsurface temperature is estimated from the climatological data, it is necessary to select the recharge area as a representative point where climatological conditions directly affect the subsurface temperature. As described in Chapter 2, though the subsurface temperature in Japan corresponds to the climatological data to some extent, the scatter of correspondence is large. This is caused by the lack of considering where the observation points are located in the groundwater flow system.

VII CONCLUSIONS

In this study, changes in subsurface temperature in time and space in the Nagaoka Plain were observed and analyzed. In the unsaturated zone, the heat transport model which contains not only heat conduction and convection but also heat exchange is indicated to explain the change in soil temperature. As the result of numerical simulation using the model, the ratios of infiltrated water to the snowmelt water and rainfall are obtained. In the saturated zone, the groundwater temperature field is clarified by measuring water temperatures in the wells. The relationship between the regional difference of subsurface temperatures and the regional groundwater flow by which the difference is caused, is clarified.

The results in this study are summarized as follows;

(1) The infiltrated meltwater makes the soil temperatures decrease at all depths in the capillary water zone in the daytime. This is caused by the movement of mobile water, pushed down by the infiltrated meltwater under a soil temperature gradient that is steep and positive downward. An increase in the soil temperature after infiltration at all depths in the capillary zone can be explained by the heat exchange between soil particles plus immobile water and mobile water.

(2) Seasonal changes in temperature-depth profiles are classified into four characteristic types. It was made

clear by the analysis using the numerical model considering heat convection that these types were caused by the regional groundwater flow. These four types were named recharge, discharge, advection and pumping types.

(3) Recharge type wells are located in the recharge area of the groundwater flow system. The depth to the isothermal layer of the recharge type profile is deeper by 5 m than the one calculated by heat conduction theory. This phenomenon can be explained by the downward groundwater flow of the order of 0.01 m/day throughout the year.

(4) Discharge type wells of temperature-depth profiles are located in the discharge area of regional groundwater system. The depth to the isothermal layer of discharge type profiles is shallower by 5 m than the one calculated by heat conduction theory. This phenomenon can be explained by the upward groundwater flow of the order of 0.01 m/day throughout the year.

(5) Temperature-depth profiles of the advection type near the Shinano River do not show a marked gradient in the vertical direction. That is to say, water temperatures of the advection type change the same way at each depth by the effect of the horizontal heat convection. Thermal diffusivity in the horizontal direction near the Shinano River was three times as large as the value of the vertical direction.

(6) Pumping type wells are located in the urban area where the groundwater level falls about 10 m caused by pumping of groundwater for snow melting during the

winter. It was caused by the downward shift of the warmer shallow water. The position and temperature of the warmer layer caused by pumping depends on the groundwater level before pumping and the falling rate of the groundwater level.

(7) The infiltration rate in the recharge area is about two times as large as that in the discharge area by the analysis of the change in groundwater temperature. The ratio of the infiltrated water to the snowmelt water is about 1.5 times as large as that of rainfall by the analysis of the change in the soil temperature.

REFERENCES

Akratanakul,S., Boersma,L. and Klock,G.O. (1983) : Sorption processes in soils as influenced by pore water velocity: 1.Theory. Soil Science, 135, 267-274.

Andrews,C.B. and Anderson,M.P. (1979) : Thermal alteration of groundwater caused by seepage from a cooling lake. Water Resour. Res., 15, 595-602.

Arai,T. (1968) : Hydro-climatological study on the mid-winter runoff from the snowy regions in Japan. Geogr. Rev. Japan, 41, 615-621.**

Bouwer,H. (1978) : "Groundwater Hydrology". McGraw-Hill, New York, 480pp.

Boyle,J.M. and Saleem,Z.A. (1979) : Determination of recharge rate using temperature depth profiles in wells. Water Resour. Res., 15, 1616-1622.

Bredehoeft, J.D. and Papadopulos, I.S. (1965) : Rates of vertical groundwater movement estimated from the earth's thermal profile. Water Resour. Res., 1, 325-328.

Carslaw,H.S. and Jaeger,J.C. (1959) : " Conduction of heat in solids, 2nd edn". Oxford Univ. Clarendon Press, U.K., 510pp.

Cartwright,K. (1968) : Thermal prospecting for groundwater. Water Resour. Res., 4, 395-401.

Cartwright,K. (1970) : Groundwater discharge in the Illinois Basin as suggested by temperature anomalies. Water Resour. Res., 6, 912-918.

Cartwright,K. (1979) : Measurement of fluid velocity using temperature profiles : Experimental verification. J. Hydrol., 43, 185-194.

Cary,J.W. (1966) : Soil moisture transport due to thermal gradients : Practical aspects. Soil Sci. Soc. Amer. Proc., 30, 428-433.

Claesson,J. (1978) : Interim Report of Dept. of Mathematical Physics and Building Science, Part 2-15, Lund, Sweden.

Combarnous, M.A. and Bories, S.A. (1975) : Hydrothermal convection in saturated porous media. Ven Te Chow ed., "Advances in Hydroscience.", 10, Academic Press, New York, 231-307.

De Vries,D.A. (1958) : Simultaneous transfer of heat and moisture in porous media. Eos Trans. Amer. Geophys. Union, 39, 909-916.

Domenico, P.A. and Palciauskas, V.V. (1973) : Theoretical analysis of forced convective heat transfer in regional groundwater flow. Geol. Soc. Amer. Bull., 84, 3803-3813.

Environmental Agency, Ministry of Construction, Niigata prefecture and Conference on water resources measures in Chuetsu (1982) : "Research on the actual condition of the groundwater pumpage". 371pp.*

Higuchi,M. (1978) : " Movement of water in an unsaturated zone ". D.Sc. Dissertation of Univ. Tsukuba, 160pp.

Hillel,D. (1971) : "Soil and water, Physical principles and processes". Academic Press, New York, 288pp.

Jury, W.A. and Miller, E.E. (1974) : Measurement of the

transport coefficients for coupled flow of heat and moisture in a medium sand. Soil Sci. Soc. Amer. Proc., 38, 551-557.

Kayane,I. (1980) : Groundwater use for snowmelting on the road. GeoJournal, 4, 173-181.

Kayane,I., Taniguchi,M. and Sanjo,K. (1985) : Alteration of the groundwater thermal regime caused by advection. Hydrol. Sci. J., 28, 125-137.

Kimball,B.A., Jackson,R.D., Reginato,R.J., Nakayama,F.S. and Idso,S.B. (1976) : Comparison of field-measured and calculated soil-heat fluxes. Soil Sci. Soc. Amer. J., 48, 18-25.

Kiuchi,S. (1950) : The study of climate under the ground : The observation on the depth and temperature of isothermal stratum in Japan and Manchuria. Geophys. Mag., 59, 28-32.**

Kobayashi,D. (1979) : Runoff of snowmelt water. Kisho-kenkyu note, 136, 39-48.*

Krige,L.J. (1939) : Borehole temperatures in the Transvaal and Orange Free State. Proc. Roy. Soc. Lond., A, 173, 450-474.

Milly, P.C.D. (1982) : Moisture and heat transport in hysteretic, inhomogeneous porous media : A matric head-based formulation and a numerical model. Water Resour. Res., 18, 489-498.

Ministry of Agriculture, Forestry and Fisheries and Meteorological Agency (1982) : "Data of soil temperature etc. part 1". 291pp.*

Ministry of Agriculture, Forestry and Fisheries and Meteorological Agency (1984) : "Data of soil temperature etc. part 2". 56pp.*

Murashita, T. (1968) : Groundwater temperature. Industry water, 118, 51-58.*

Nagaoka Construction Office (1975) : "Report on construction of observation wells". Ministry of Construction, 259pp.*

Nishizawa,T. and Hasegawa,T. (1969) : Soil temperature in Japan. Geogr. Rev. Japan, 42, 775-777.**

Ohwada, M. (1969) : Distribution of the soil temperature in Japan. Geogr. Rev. Japan, 42, 138-144.**

Parsons,M.I. (1970) : Groundwater thermal regime in a glacial complex. Water Resour. Res., 6, 1701-1720.

Philip,J.R. and De Vries,D.A. (1957) : Moisture movement in porous materials under temperature gradients, Eos Trans. Amer. Geophys. Union, 38, 222-232.

Sakura, Y. (1977) : A method for estimating groundwater velocity from temperature data. Water Temp. Res., 21, 2-14.*

Sakura, Y. (1978) : Study on groundwater cycle by water temperature. Ichikawa,M. and Kayane,I. eds., "Water balance in Japan"., Kokon Shoin, Tokyo, 344pp.*

Sakura,Y. (1984) : Change of thermal regime in surface soil layer during a heavy rain. Geogr. Rev. Japan, 57, 628-638.**

Sakura,Y. and Taniguchi,M. (1983) : Experiments of rain infiltration on characteristics of soil water movement using a soil column. Geogr. Rev. Japan, 56, 81-93.**

Sarson, P.B. (1960) : Exceptional sudden changes of earth temperature. Met. Mag., 89, 201-209.

Shul'gin, A.M. (1957) : "The temperature regime of soils". (Transported from Russian by Gourevitch,A.,1965), Sivan Press, Jerusalem, 210pp.

Smettem,K.R.J. (1984) : Soil-water residence time and solute uptake,3. Mass transfer under simulated winter rainfall conditions in undisturbed soil cores. J. Hydrol., 67, 235-248.

Sophocleous,M. (1979) : Analysis of water and heat flow in unsaturated-saturated porous media. Water Resour. Res., 15, 1195-1206.

Sorey, M.L. (1971) : Measurement of vertical groundwater velocity from temperature profiles in wells. Water Resour. Res., 7, 963-970.

Stallman,R.W. (1963) : Computation of groundwater velocity from temperature data, U.S. Geol. Surv. Water Supply Pap., 1544-H, 36-46.

Stallman, R.W. (1965) : Steady one-dimensional fluid in a semi-infinite porous medium with sinusoidal surface temperature. J. Geophys. Res., 70, 2821-2827.

Suzuki,S. (1960) : Percolation measurements based on heat flow through soil with special reference to paddy fields. J. Geophys. Res., 65, 2883-2885.

Takahashi, M. (1967) : On the ground-water temperature in Japan. Geol. Surv. Japan, 219, 1-41.*

Tanaka,T., Kayane,I. and Tase,N. (1979) : Shousetsu pipe in Nagaoka (1) - Occurrence of groundwater and groundwater

use. Presented at Ann. Meetg., Asoc. Japan. Geogr., 17, 34-35.*

Taniguchi,M. (1985) : Effects of snow cover and infiltrated meltwater on soil and groundwater temperature in and around Nagaoka city. Geogr. Rev. Japan, 58, 370-384.**

Taniguchi, M. and Kayane, I. (1986) : Changes in soil temperature caused by infiltration of snowmelt water. I.A.H.S. Publ., 155, 93-101.

Taniguchi,M., Sakura,Y. and Kotoda,K. (1982) : Measurements of water flux by microflowmeter. Bull. Environ. Res. Center, Univ. Tsukuba, 6, 87-92.*

Taniguchi,M., Sanjo,K. and Kayane,I. (1984) : Importance of groundwater temperature in groundwater survey. Hydrology, 14, 50-60.**

Todd, D.K. (1959) : "Groundwater hydrology". John Wiley, London, 535pp.

Trudgill,S.T., Pickles,A.M. and Smettem, K.R.J. (1983) : Soil-water residence time and solute uptake : 2. Dye tracing and preferential flow predictions. J. Hydrol., 62, 279-285.

Van Genuchten,M.Th. and Wierenga,P.J. (1976) Mass transfer studies in sorbing porous media, I. Analytical solutions. Soil Sci. Soc. Amer. J., 40, 473-480.

Wierenga, O.J., Hagan, R.M. and Nielsen D.R. (1970) : Soil temperature profiles during infiltration and redistribution of cool and warm irrigation water. Water Resour. Res., 6, 230-238.

Wilkinson,G.E. and Klute,A. (1962) : The temperature effect

on the equilibrium energy status of water held by porous media. Soil Sci. Soc. Amer. Proc., 26, 326-329.

Yamaguchi,K. (1966) : Water temperature. Aki,K. and Tada,F. eds., "Handbook of water resources.", Asakura Shoten, Tokyo, 659pp.*

Yokoyama,T., Umemiya,H. and Abiko,H. (1975) : Heat exchange of storage type through underground strata by artificial recharge. J. Jap. Assoc. Groundwater Hydrology, 17, 55-67.**

Yusa,Y. (1981) : A model of soil temperature distribution in geothermal area. Water Tem. Res., 24, 37-43.*

* in Japanese

** in Japanese with English abstract